AD_____

Award Number: W81XWH-09-1-0184

TITLE: Defining theRole of BTLA in Breast Cancer Immunosurveillance and Selective Targeting of the BTLA-HVEM-LIGHT Costimulatory System

PRINCIPAL INVESTIGATOR: William E. Gillanders, M.D.
Kenneth M. Murphy, M.D.

CONTRACTING ORGANIZATION: Washington University
St. Louis, MO 63130

REPORT DATE: May 2011

TYPE OF REPORT: Annual

PREPARED FOR: U.S. Army Medical Research and Materiel Command
Fort Detrick, Maryland 21702-5012

DISTRIBUTION STATEMENT: Approved for Public Release;
Distribution Unlimited

The views, opinions and/or findings contained in this report are those of the author(s) and should not be construed as an official Department of the Army position, policy or decision unless so designated by other documentation.

REPORT DOCUMENTATION PAGE

Form Approved
OMB No. 0704-0188

Public reporting burden for this collection of information is estimated to average 1 hour per response, including the time for reviewing instructions, searching existing data sources, gathering and maintaining the data needed, and completing and reviewing this collection of information. Send comments regarding this burden estimate or any other aspect of this collection of information, including suggestions for reducing this burden to Department of Defense, Washington Headquarters Services, Directorate for Information Operations and Reports (0704-0188), 1215 Jefferson Davis Highway, Suite 1204, Arlington, VA 22202-4302. Respondents should be aware that notwithstanding any other provision of law, no person shall be subject to any penalty for failing to comply with a collection of information if it does not display a currently valid OMB control number. **PLEASE DO NOT RETURN YOUR FORM TO THE ABOVE ADDRESS.**

1. REPORT DATE	2. REPORT TYPE	3. DATES COVERED
May 2011	Annual	1 May 2010 – 30 April 2011

4. TITLE AND SUBTITLE

Defining theRole of BTLA in Breast Cancer Immunosurveillance and Selective Targeting of the BTLA-HVEM-LIGHT Costimulatory System

5a. CONTRACT NUMBER

5b. GRANT NUMBER
W81XWH-09-1-0184

5c. PROGRAM ELEMENT NUMBER

6. AUTHOR(S)

William Gillanders
Kenneth Murphy

E-Mail: gillandersw@wudosis.wustl.edu

5d. PROJECT NUMBER

5e. TASK NUMBER

5f. WORK UNIT NUMBER

7. PERFORMING ORGANIZATION NAME(S) AND ADDRESS(ES)

Washington University
St. Louis, MO 63130

8. PERFORMING ORGANIZATION REPORT NUMBER

9. SPONSORING / MONITORING AGENCY NAME(S) AND ADDRESS(ES)
U.S. Army Medical Research and Materiel Command
Fort Detrick, Maryland 21702-5012

10. SPONSOR/MONITOR'S ACRONYM(S)

11. SPONSOR/MONITOR'S REPORT NUMBER(S)

12. DISTRIBUTION / AVAILABILITY STATEMENT
Approved for Public Release; Distribution Unlimited

13. SUPPLEMENTARY NOTES

14. ABSTRACT

None provided.

15. SUBJECT TERMS
None provided.

16. SECURITY CLASSIFICATION OF:			17. LIMITATION OF ABSTRACT	18. NUMBER OF PAGES	19a. NAME OF RESPONSIBLE PERSON
a. REPORT	b. ABSTRACT	c. THIS PAGE			USAMRMC
U	U	U	UU	51	19b. TELEPHONE NUMBER *(include area code)*

TABLE OF CONTENTS

INTRODUCTION 4

BODY 6

KEY RESEARCH ACCOMPLISHMENTS 9

REPORTABLE OUTCOMES 10

CONCLUSIONS 11

APPENDICES 12

Appendix #1: Establishment of a BALB/c-*neu*T/BTLA$^{-/-}$ colony for studies of breast cancer immunosurveillance 13

Appendix #2: Generation and validation of wildtype and mutant HVEM constructs 14

Appendix #3: Functional analysis of wildtype and mutant HVEM in the context of DNA vaccination 19

Appendix #4: Establishment and validation of a clinically relevant breast cancer vaccine model 20

Appendix #5: Defining the role of BTLA in the context of graft-versus-host disease 21

Appendix #6: Defining the mechanisms of antigen presentation and specific dendritic cell subsets following DNA vaccination 31

INTRODUCTION

BACKGROUND: In the last decade, considerable progress has been made in understanding the complex regulatory networks that control immune responses. Regulating the extent, quality and duration of immune responses is critical for balancing protective immunity and tissue injury. Costimulatory (CD28, ICOS) and inhibitory (CTLA4, PD-1) molecules of the CD28 receptor family provide critical secondary signals regulating this balance, and recent work has uncovered critical roles for CTLA4 and PD-1 in restraining immune responses in chronic viral infection and malignancy. We recently cloned B- and T-lymphocyte attenuator (BTLA), the third inhibitory receptor of the CD28 family expressed on lymphocytes. Using BTLA-deficient mice and monoclonal antibodies specific for BTLA that we generated, we have studied several in vivo models of infection and autoimmunity, showing the importance of BTLA in regulating immune responses. Several lines of evidence suggest that inhibitory molecules such as CTLA-4 and PD-1 limit cancer immunosurveillance.

OBJECTIVE/HYPOTHESIS: The hypothesis of this application is that BTLA contributes to the inhibition of breast cancer immunosurveillance, and selective targeting of the BTLA-LIGHT-HVEM costimulatory system can enhance breast cancer immunity.

SPECIFIC AIMS:

(1) Define the role of BTLA in breast cancer immunosurveillance.

(2) Determine if inhibitory molecules of the CD28 receptor family function as redundant immunologic checkpoints in breast cancer immunosurveillance.

(3) Develop novel therapeutics to successfully dissociate T cell costimulation and inhibition in the BTLA-LIGHT-HVEM costimulatory system.

PROGRESS: The award was in the format of a Synergistic Idea Award to William E. Gillanders, M.D., a breast cancer surgeon, and Kenneth Murphy, M.D., Ph.D., a basic immunologist. The current reporting period represents the second year of a two year award. Of note, Dr. Gillanders has requested a no-cost extension to continue the studies proposed.

The research proposed in Specific Aims 1 and 2 is focused on the role of BTLA in breast cancer immunosurveillance and relies heavily on genetically engineered mice that spontaneously develop breast cancer (BALB/c-neuT mice). These mice are currently being expanded and bred to gene-deficient mice to definitively evaluate the role of BTLA in this process. Although using genetically engineered mice that spontaneously develop breast cancer has a number of advantages, these studies require an initial investment in time to establish mice on the desired genetic background, and to establish cohorts of mice that will develop breast cancers at 25-30 weeks of age. These experiments are currently ongoing, and the funds in the no-cost extension are supporting this work.

The main focus of Specific Aim 3 is on selective targeting of the BTLA-LIGHT-HVEM costimulatory system. We have generated wildtype and mutant HVEM constructs, and tested these constructs in a DNA vaccine model. We have made the surprising observation that wildtype HVEM can enhance the immune response following DNA vaccination, and this effect is BTLA-dependent. Mechanistic studies are currently ongoing to follow-up on this surprising observation.

Finally, the Synergistic Idea Award has resulted in a successful and productive collaboration between Drs. Murphy and Gillanders. In collaboration, we have made important insights into BTLA biology, and defined the ability of an agonist BTLA antibody to prevent graft-versus-host disease. In addition, we have made important contributions to the understanding of antigen presentation and the role of specific dendritic cell subsets following DNA vaccination.

BODY

Specific Aims 1A, 1C, 2A, 2B: The studies outlined in these Aims are underway. Our BALB/c-*neu*T and related breeding colonies had to be re-established, causing a significant delay in establishing the BALB/c-*neu*T/BTLA$^{-/-}$ colony. We currently have successfully expanded our colony of BALB/c-*neu*T mice to over seven breeding pairs, and the BALB/c-*neu*T/BTLA$^{-/-}$ colony is currently being re-established. Cohorts of BALB/c-*neu*T/BTLA$^{-/-}$ mice will be evaluated when sufficient animals are available at the appropriate age (25-30 weeks). Please see Appendix #1 for additional details. No spontaneous tumors from BALB/c-*neu*T mice have been evaluated to date as animals of sufficient age and appropriate genetic background are not yet available.

Specific Aims 3A, 3B: LIGHT signaling through HVEM results in CD28-independent T cell costimulation, dramatically enhancing antitumor and other cell-mediated immune responses, whereas BTLA signaling through HVEM induces inhibitory signals. We successfully created wildtype HVEM, and three different HVEM mutants using site-directed mutagenesis: P17A, Y23A, and V36A. These mutations have been shown previously to ablate binding of BTLA but preserve binding of LIGHT. The mutant constructs were initially expressed in CHO cells to assess binding of HVEM and BTLA. Subsequently, the mutant constructs were cloned into pcDNA3 vector for further functional validation. *In vitro* studies confirm that the P17A mutation successfully ablates the interaction between HVEM and BTLA. Please see Appendix #2 for additional details.

Specific Aim 3C: Wildtype (wt) and mutant HVEM constructs were successfully cloned into the pcDNA3 plasmid DNA vector, and expression was confirmed. To assess the ability of wildtype and mutant HVEM molecules to enhance DNA vaccination, several vaccination protocols were developed based on the model antigen, ovalbumin (OVA). Surprisingly, preliminary data suggest that wildtype, but not mutant HVEM, is an effective molecular adjuvant in the context of DNA vaccination. Please see Appendix #3 for additional details.

To confirm and extend these findings, we have established and validated a clinically relevant breast cancer vaccine model in our laboratory to test the HVEM constructs. This model system is based on the BALB/c-*neu*T genetically engineered murine model of breast cancer. BALB/c-*neu*T mice express the transforming rat oncogene HER2/neu under the mouse mammary tumor virus (MMTV) promoter. These mice spontaneously develop breast cancer with a well-defined progression from dysplasia, to *in situ* carcinoma, to overt invasive carcinoma similar to human disease. We have established a cancer vaccine model, where DNA vaccination with conventional (HER2/neu cDNA vaccine), or experimental (HER2/neu single chain trimer DNA vaccines) cancer vaccines can protect against tumor challenge with a HER2/neu-expressing tumor. This represents an ideal platform for additional testing of the wildtype and mutant HVEM constructs. Please see Appendix #4 for additional details.

Additional Studies resulting from the collaboration: Given the surprising results noted above (Specific Aim 3C), additional mechanistic studies of BTLA biology have been performed in the Murphy/Gillanders laboratory, pending availability of BALB/c-*neu*T/BTLA$^{-/-}$ mice of the appropriate age and genetic background. These

studies of the BTLA-LIGHT-HVEM costimulatory system have been carried out in a murine model of graft-versus-host disease. Based upon the likely similarity of the mechanisms of action of BTLA in breast cancer-specific T cells and in expanding T cells in the GVHD model, we have carried out a series of studies into the mechanism and effects of BTLA-directed immunotherapy. In GVHD, T cells expanding following bone marrow transplantation not only manifest graft-versus-host disease, but also mediate important antitumor effects. Therefore, we have carried out an analysis to evaluate the role of BTLA-directed therapy in this setting. The model used is the fully irradiated GVHD model. Two forms of this were tested, including a fully MHC-mismatched model of B6 transfer into BALB/c recipients, or a parental into F1 model. In both cases, either lethal or chronic GVHD is established, concurrent with significant weight loss, and a permanent mucosal inflammatory disease in the gut and elsewhere. Our essential finding is that the treatment of recipient mice with a single injection of anti-BTLA antibody (6A6) results in permanent prevention of GVHD. Since last year's report, we have further identified that the mechanism of anti-BTLA treatment at the time of bone marrow transplantation is a selective blockade of alloreactive donor T cells, without a blockade in the expansion and effector activities of normally protective and pathogen-specific donor T cells. This work has now been published in the *Journal of Experimental Medicine*. Of relevance to the current proposal, we have found that HVEM is not involved in the mechanisms of the beneficial effects of BTLA-directed therapy. During homeostatic expansion, HVEM is not engaged to limit the expansion of effector T cells after BMT. This observation may alter our future focus to concentrate on BTLA rather than HVEM manipulations in considering ways to augment anti-tumor vaccinations. Please see Appendix #5 for additional details (reprint of manuscript published in Journal of Experimental Medicine).

In order to define the mechanism of action of wildtype HVEM in DNA vaccination (Specific Aim 3C), we have performed additional studies to define the mechanisms of antigen presentation and specific dendritic cell subsets following DNA vaccination. Previous studies suggest that DNA vaccines may activate CTL by the direct transfection of dendritic cells (direct priming). In contrast, other studies suggest that non-immune cells are transfected, and antigens are subsequently processed and presented by dendritic cells to activate CTL (cross-presentation). Importantly, only certain immune cells, such as certain $CD8\alpha^+$ and $CD103^+$ lineages of dendritic cells, are efficient in cross-presentation, and strategies to optimize DNA-based vaccines depend critically on the mechanism(s) of antigen presentation and specific dendritic cell subtypes involved. We recently generated $Batf3^{-/-}$ mice which lack development of the $CD8\alpha^+$ and $CD103^+$ lineages of dendritic cells, allowing us to test the role of these dendritic cell subtypes and cross-presentation in CTL priming following DNA vaccination. We have determined that CTL activation is selectively ablated in $Batf3^{-/-}$ mice following DNA vaccination. These data provide the strongest evidence to date that cross-presentation and $CD8\alpha^+$ dendritic cells are required for the generation of effective CTL immunity following DNA vaccination, with important implications for the rational development of DNA vaccines. Please see Appendix #6 for additional details (text of manuscript submitted for publication).

Problem Areas: We encountered an unforeseen problem when the postdoctoral fellow recruited to work on this project left unexpectedly due to family health issues. This individual ultimately resigned the position, and this unexpected departure ultimately resulted in having to re-establish the BALB/c-neuT and related mouse colonies. We have now successfully recruited another postdoctoral fellow to fill the position. This individual has a strong background in tumor immunology and vaccine development. In addition, we have recruited a second postdoctoral fellow to work on this project. This individual has obtained a postdoctoral fellowship award from the Swiss National Foundation, and the main focus of her proposed research is the studies described in Specific Aims 1 and 2 of this proposal.

KEY RESEARCH ACCOMPLISHMENTS

(1) Generation of proposed genetic strains is completed or underway.

(2) Successful creation of wildtype and mutant HVEM constructs, and successful cloning of these constructs into retroviral and plasmid DNA vectors.

(3) Initial assessment of the adjuvant effect of wildtype and mutant HVEM constructs as novel molecular adjuvants in a DNA vaccine model. Wildtype HVEM does appear to be an effective molecular adjuvant.

(4) Successful establishment and validation of a clinically relevant breast cancer DNA vaccine model, representing an ideal platform for testing the wildtype and mutant HVEM constructs.

(5) Identification of an effect of BTLA-directed therapy in the treatment of graft-versus-host disease, which may have important clinical relevance in breast cancer and other diseases.

(6) Demonstration that CD8α dendritic cells, and cross-presentation, are essential for priming CD8 T cell responses following DNA vaccination.

REPORTABLE OUTCOMES

The manuscript: "Targeting of B and T lymphocyte associated (BTLA) prevents graft-versus-host disease without global immunosuppression" was published in the *Journal of Experimental Medicine* (JEM 2010, 207:2552). Please see Appendix #5.

CONCLUSIONS

Progress has been made towards the goal of defining the role of BTLA in breast cancer immunosurveillance. Analysis of spontaneous breast cancers in mice of the appropriate age and genetic background will be required to complete Specific Aims 1 and 2 of the proposal.

We have successfully targeted the BTLA-LIGHT-HVEM costimulatory system, demonstrating that wildtype HVEM can be used as a novel molecular adjuvant to enhance the immune response following DNA vaccination.

Mechanistic studies in a model of graft-versus-host disease confirm the importance of BTLA, and reveal a potent effect of an agonist BTLA antibody. These studies have important clinical implications for the treatment of breast cancer. Additional mechanistic studies focused on the role of mutant HVEM as a molecular adjuvant demonstrate the critical role of $CD8\alpha^{+}$ dendritic cells in the response to DNA vaccination.

APPENDICES

Appendix #1: Establishment of a BALB/c-*neu*T/BTLA$^{-/-}$ colony for studies of breast cancer immunosurveillance

Appendix #2: Generation and validation of wildtype and mutant HVEM constructs

Appendix #3: Functional analysis of wildtype and mutant HVEM in the context of DNA vaccination

Appendix #4: Establishment and validation of a clinically relevant breast cancer vaccine model

Appendix #5: Defining the role of BTLA in the context of graft-versus-host disease

Appendix #6: Defining the mechanisms of antigen presentation and specific dendritic cell subsets following DNA vaccination

Appendix #1: Establishment of a BALB/c-*neu*T/BTLA$^{-/-}$ colony for studies of breast cancer immunosurveillance

BALB/c-neuT mice were obtained from Eli Gilboa at the University of Miami on two separate occasions. BALB/c-neuT mice from this breeding colony are heterozygous for the neuT transgene, and this remains true in our breeding colony. At each generation, mice must be screened for the presence of the neuT transgene. A PCR-based genotyping reaction was developed to assess for the presence of the neuT transgene (please see below). BTLA-deficient mice on the BALB/c background were generated in the Murphy Laboratory. BALB/c-neuT x BTLA$^{-/-}$ F1 mice are screened for the presence of the neuT transgene. Transgene-positive animals are then backcrossed (F2 generation) to BTLA-/- mice to obtain neuT^{+}, BTLA$^{-/-}$ mice.

PCR Primers for genetyping neuT are: BRL R3 DIR (neu dir): 5'-GTAACACAGGCAGATGTAGGA-3'; MTV RI REV (neu rev): 5'-ATCGGTGATGTCGGCGATAT-3'; β casein (dir): 5'-GATGTGCTCCAGGCTAAAGTT-3'; β casein (rev): 5'-AGAAACGGAATGTTGTGGAGT-3'. Primers to amplify β Casein are used as a positive control, and a no template control is also used (water). The amplification program was performed in a PTC-200 Peltier thermal cycler, and included an initial denaturation at 94°C for 1 min; 35 cycles of 94°C for 1 min, 55°C for 1 min and 72°C for 2 min, and a final incubation at 72°C for 7 min. Each experiment included 5 µL of Bench Top 100 bp DNA ladder (Promega).

Using this protocol, three mice of a BTLA$^{-/-}$ x *neu*T cross were tested, and one was found to be positive for both BTLA-deficiency and expression of *neu*T (lane 2, faint band). We currently are using this mouse as a breeder in order to generate more BTLA$^{-/-}$ x *neu*T mice for future experiments.

β Casein (525 bp)

neuT transgene(230 bp)

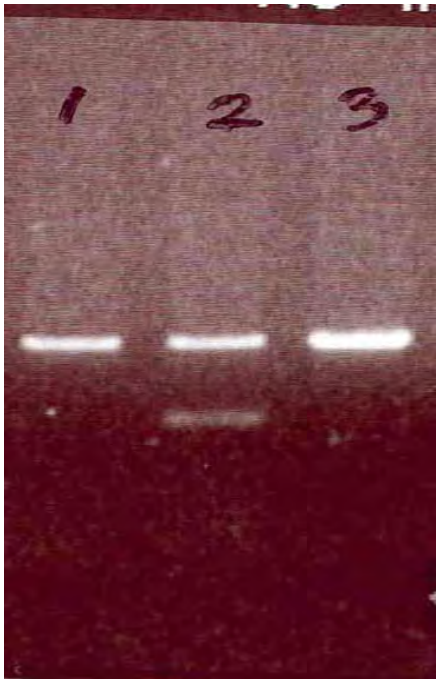

Appendix #2: Generation and validation of wildtype and mutant HVEM constructs

Goal: Introduce three HVEM mutations into the HVEM-IRES-GFP-RV vector (P17A, Y23A, V36A).

HVEM
275 aa

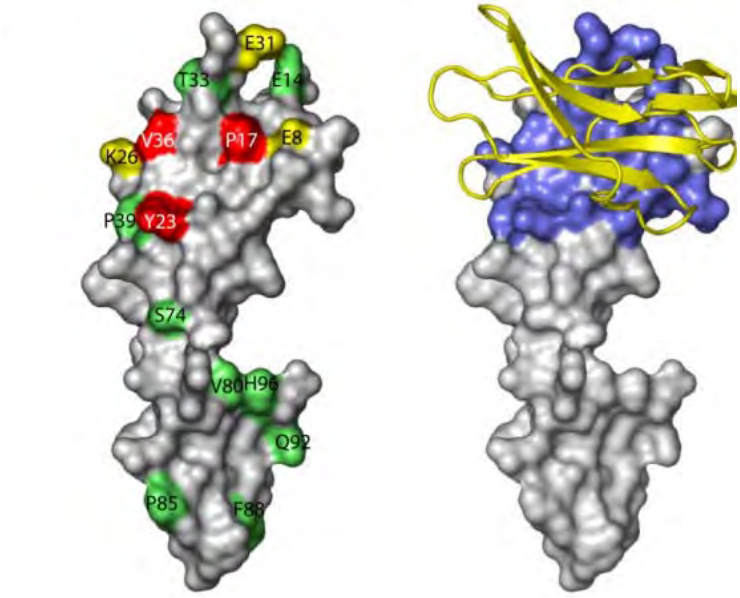

The schematic diagram above shows the position of the HVEM mutants in the HVEM protein. We performed site-directed mutagenesis PCR to amplify HVEM mutants by using HVEM wildtype as a template (HVEM in retroviral vector). Primers used to amplify HVEM mutants (P17A, Y23A, and V36A) are listed below.

Alanine-scanning mutagenesis of HVEM. Mutated residues that reduced BTLA binding > 5-fold (red) are the points we mutated in our HVEM mutants.

HVEM SDM Primers

mP17AFP GACGAGTGCTGCGCCATGTGCAACCCA

mP17ARP TGGGTTGCACATGGCGCAGCACTCGTC

mY23AFP GCAACCCAGGTGCCCATGTGAAGCAGG

mY23ARP CCTGCTTCACATGGGCACCTGGGTTGC

mV36AFP TACAGGCACAGCCTGTGCCCCCTGTCC

mV36ARP GGACAGGGGGCACAGGCTGTGCCTGTA

PCR reactions were performed according to the manufacturer's instructions (Quick-change Lightning Site-Directed Mutagenesis kit from Stratagene). The amplification program was performed in a PTC-200 Peltier thermal cycler, and included an initial denaturation at 95°C for 2 min; 18 cycles of 95°C for 20 sec, 60°C for 10 sec and 68°C for 3 min 30 sec, and a final incubation at 68°C for 5 min. Transformation was performed immediately following PCR. Briefly, 2 µL of DpnI was aliquoted into each vial containing PCR product (50 µL), incubated at 37 °C for 5 min, then 45 µL of XL10 gold ultracompetent cells (XL10G) and 2 µL of β-ME mix were added, and the contents of the tube were swirled gently, and incubated on ice for 2 min. 2 µL of the DpnI-treated DNA from each sample was then transferred to separate aliquots of XL10 G cells, mixed gently and incubated on ice for 30 minutes, followed by a 42 second-heat pulse, then incubated in tubes on ice for 2 minutes. 0.5 mL of preheated NZY+ broth was then added to each tube, and the tubes were incubated at 37°C for 1 hour with shaking at 225-250 rpm. 100 µL of each transformation reaction was then plated on an agar plate containing Amp for the plasmid vector.

The figure below demonstrates the plasmid containing the wildtype and mutant HVEM-IRES-GFP constructs:

HVEM-IRES-GFP-RV (7286 bp)

Constructs were tested by restriction enzyme digest and selected constructs were sent for sequencing to confirm mutations. After confirmation by sequencing, constructs were extracted using a maxi prep kit from Sigma Aldrich.

In order to determine if the wildtype and mutant HVEM constructs can be expressed *in vitro*, we transfected CHO cells with the wildtype and mutant HVEM constructs. GFP expression was assessed using a fluorescence microscope 48 hours after transfection. Subsequently, the transfected CHO cells were stained with HVEM antibody and/or BTLA tetramer followed by flow cytometry. While the wildtype and mutant HVEM constructs in retroviral vectors were prepared in the first year of the award, these key experiments to test construct expression were performed by the new postdoctoral fellow in the second year of the award.

The binding studies demonstrated that binding of BTLA is ablated in the P17A HVEM mutant, whereas binding is intact in the V36A mutant and wildtype HVEM. The Y23A mutation reduced BTLA binding by ~50% (please see below).

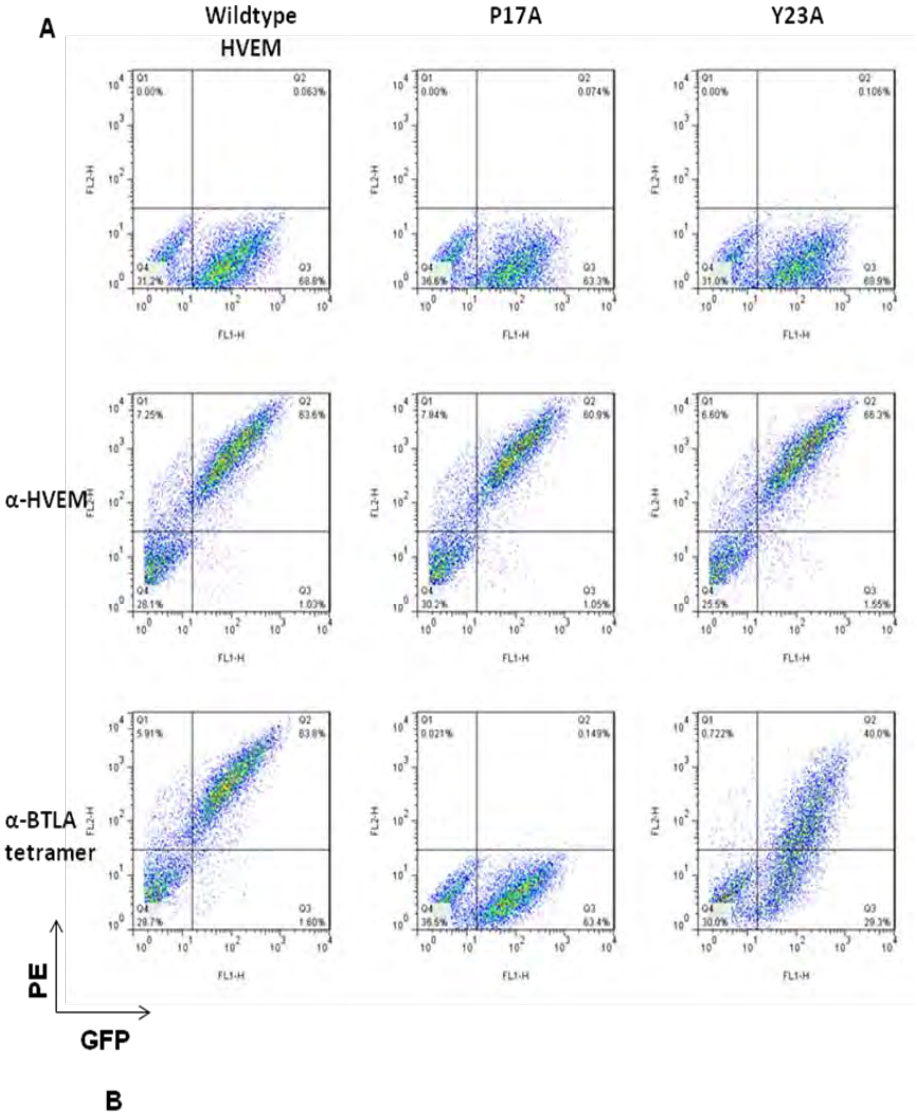

B

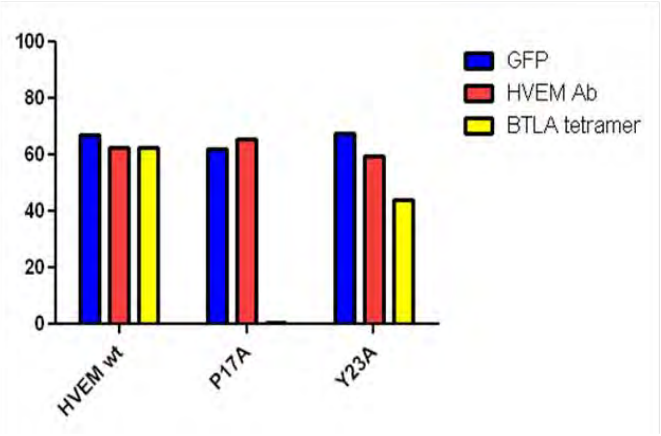

Wildtype and mutant HVEM constructs were cloned into retroviral vectors as detailed above. CHO cells were transduced with the indicated constructs, and then stained with PE-conjugated α-HVEM Ab (second row), or PE-conjugated α-BTLA tetramer (third row), and analyzed by flow cytometry. (A) Wildtype and mutant HVEM expression on CHO cells. (B) Summary of FACS staining.

To test the wildtype and mutant HVEM constructs in a DNA vaccine model, the constructs were cloned into the pcDNA3 vector. Two series of constructs were generated, one series with GFP (for *in vitro* studies) and one without GFP (for DNA vaccine studies), and expressed in 293 cells. Flow cytometry was performed to assess expression of GFP and HVEM.

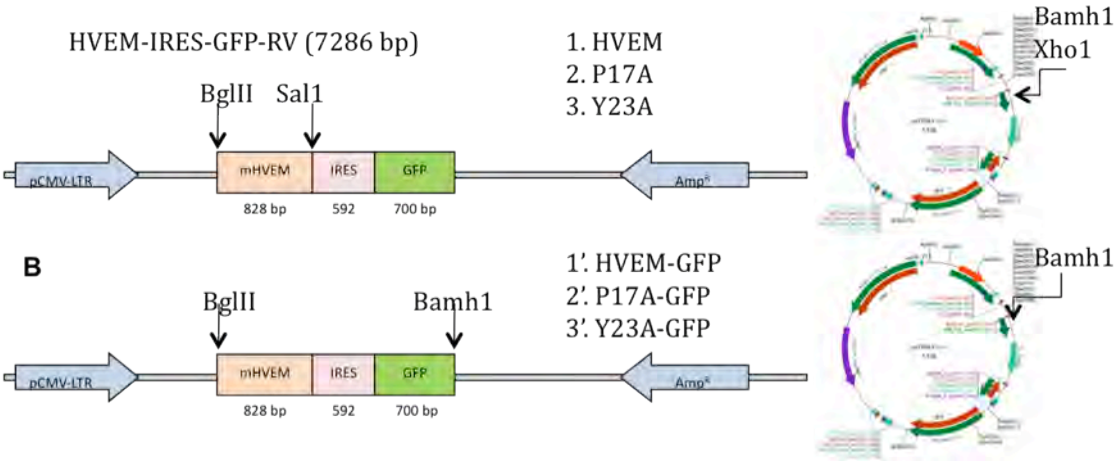

(A, B) Cloning strategy for wildtype and mutant HVEM constructs (P17A, Y23A). All constructs were initially generated by site-directed mutagenesis and cloned into retroviral vectors (shown on left). The constructs were subsequently cloned into pcDNA3 plasmid constructs (shown on right). (A) Wildtype and mutant HVEM constructs were cloned into pcDNA3 without GFP. These constructs are used as molecular adjuvants in DNA vaccine studies. (B) Wildtype and mutant HVEM constructs were cloned into pcDNA3 with GFP for *in vitro* validation studies.

Once the pcDNA3 constructs were validated by restriction digest and sequencing, they were transfected into 293T cells and tested for expression in flow cytometry analyses. Please see below.

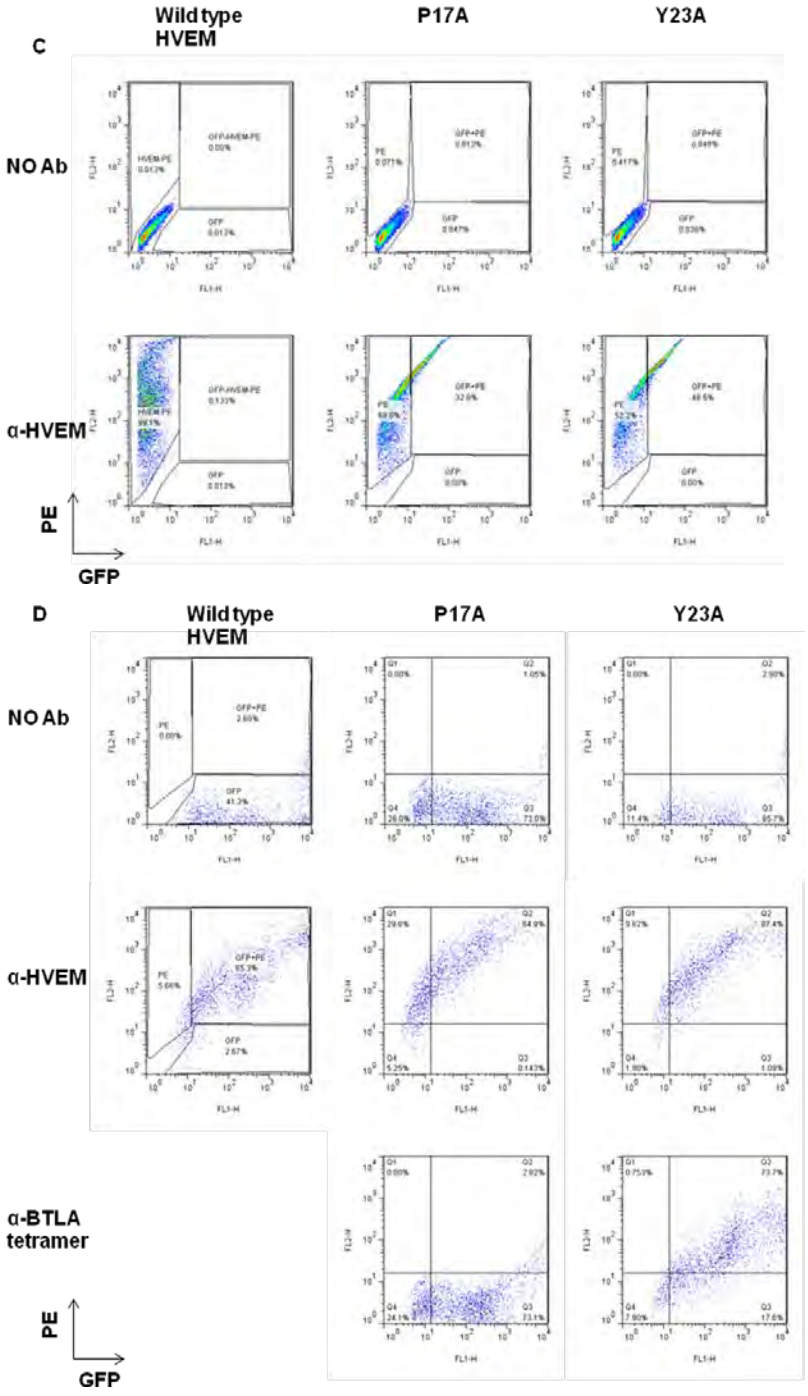

(C) Expression of wildtype and mutant HVEM in 293T cells. (D) Expression of wildtype and mutant HVEM with GFP in 293T cells. All constructs stain positive for HVEM, but the P17A mutation completely ablates BTLA binding, and the Y23A mutation partially ablates BTLA binding.

These data show that the wildtype and mutant HVEM constructs are expressed and can be recognized by HVEM-specific antibodies. They also confirm the P17A mutation completely abrogates BTLA binding *in vitro*, whereas the Y23A mutation partially abrogates BTLA binding.

Appendix #3: Functional analysis of wildtype and mutant HVEM in the context of DNA vaccination

To assess if HVEM mutants can enhance the immune response to DNA vaccination, ovalbumin (OVA) cDNA was administered by gene gun with or without wildtype and mutant HVEM constructs. We typically vaccinate mice three times at days 0, 3, and 6, either by gene gun, and assess the primary immune response on day 11 by ELISPOT assay using splenocytes (see below).

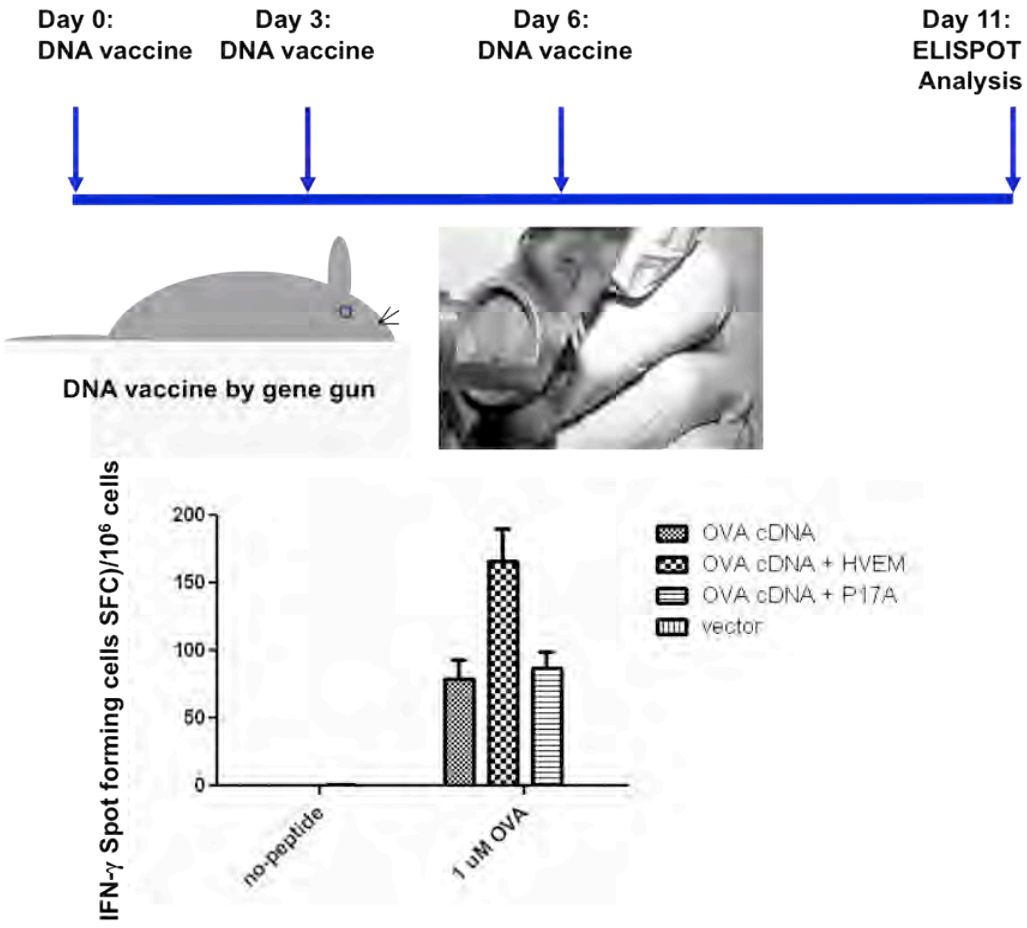

Mice were immunized by gene gun on days 0, day 3 and day 6 with OVA cDNA, OVA cDNA plus HVEM or OVA cDNA plus mutant HVEM P17A. IFN-γ ELISPOT was performed on day 11. Data shown is representative of three independent experiments. Wildtype, but not mutant HVEM enhances the $CD8^+$ T cell response to ovalbumin.

In three independent experiments, administration of wildtype HVEM enhances the immune response to OVA cDNA. However, unlike wildtype HVEM, the P17A mutant HVEM did not enhance vaccine efficacy.

We are currently repeating the experiments using an electroporation device, in a more clinically relevant breast cancer model. Specifically, we will combine wildtype or mutant HVEM with breast cancer vaccines, such as neuT cDNA or a single chain trimer DNA vaccine targeting neuT. These experiments have just been initiated and the results are pending.

Appendix #4: Establishment and validation of a clinically relevant breast cancer vaccine model

While waiting for sufficient numbers of BALB/c-*neu*T mice, we initiated DNA vaccination experiments using the BALB/c mouse breast cancer carcinoma, TUBO. TUBO is a transplantable tumor line that originates from a BALB/c-*neu*T mouse. TUBO expresses neuT, and DNA vaccination against neuT induces TUBO cell rejection. We assessed the efficacy of various neuT DNA vaccines in wild type BALB/c mice challenged with TUBO. In addition to neuT cDNA, we tested two single chain trimer (SCT) constructs expressing immunodominant epitopes of neuT. The SCT DNA constructs encode H-2K^d or H-2L^d, β_2-microglobulin, and the neuT K^d-binding peptide p66-74 (TYVPANASL) or L^d-binding peptide p162-170 (NPQLCYQDM), respectively. Both neuT cDNA and SCT DNA vaccination protected against a lethal challenge of TUBO. The data from the SCT DNA vaccination suggest that neu-specific CD8 T cells were elicited and were capable of rejecting TUBO.

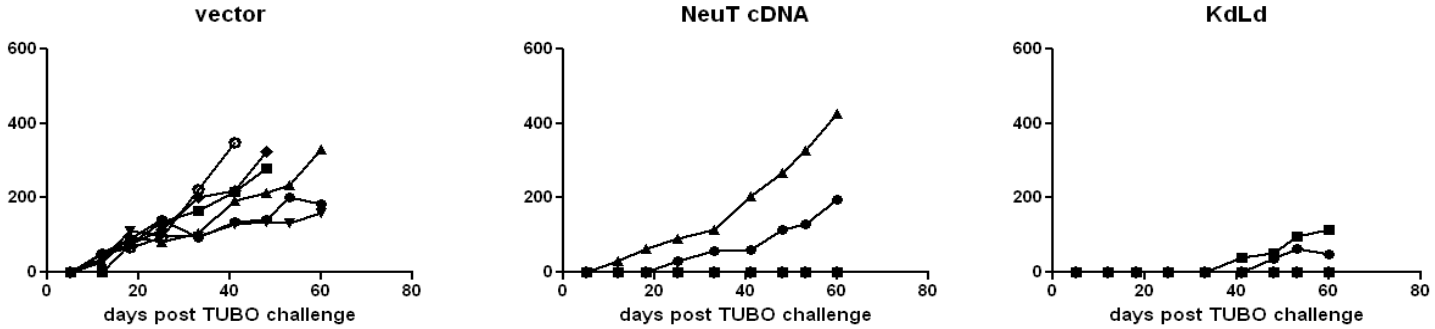

Wild type BALB/c mice (7 per group) were vaccinated on days 0, 3, and 6 by electroporation. On day 37 post immunization, mice were challenged by subcutaneous injection of TUBO (3x105/mouse). Tumor growth was measured every three days using calipers.

To further assess the peptide-specific response elicited by SCT DNA vaccination, ELISPOT assays were performed on splenocytes from vaccinated mice post vaccination.

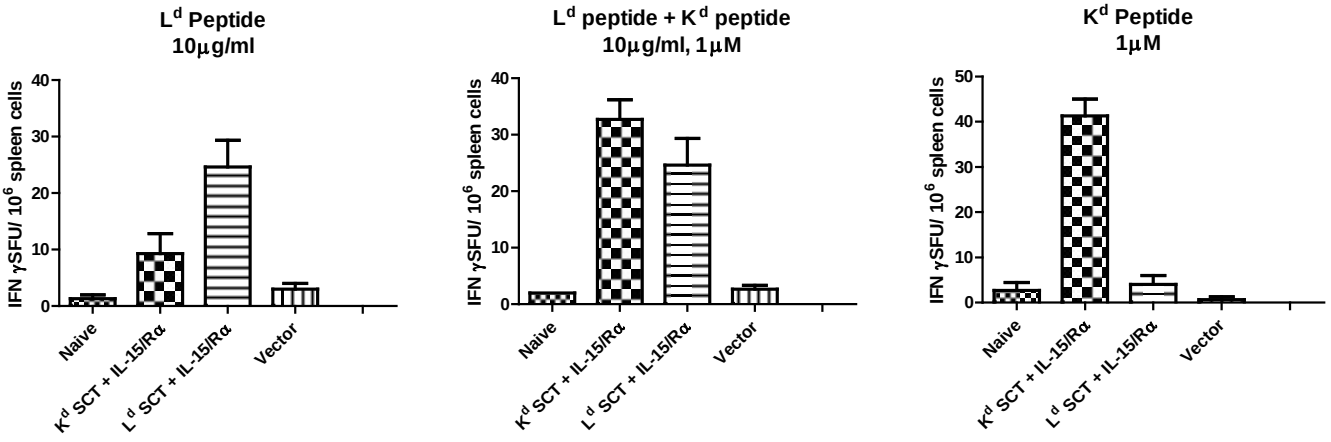

BALB/c mice (3 per group) were vaccinated on days 0, 3, and 6 by electroporation using empty vector DNA or SCT DNA, as indicated plus adjuvant (genetic constructs encoding IL-15 and IL-15Rα). On day 11, ELISPOT assays were performed on isolated splenocytes pulsed with the respective peptides encoded by the SCT constructs.

Appendix #5: Defining the role of BTLA in the context of graft-versus-host disease

Published November 15, 2010

Targeting of B and T lymphocyte associated (BTLA) prevents graft-versus-host disease without global immunosuppression

Jörn C. Albring,[1,2] Michelle M. Sandau,[1] Aaron S. Rapaport,[1] Brian T. Edelson,[1] Ansuman Satpathy,[1] Mona Mashayekhi,[1] Stephanie K. Lathrop,[3] Chyi-Song Hsieh,[3] Matthias Stelljes,[4] Marco Colonna,[1] Theresa L. Murphy,[1] and Kenneth M. Murphy[1,2]

[1]Department of Pathology and Immunology, [2]Howard Hughes Medical Institute, and [3]Department of Medicine, Division of Rheumatology, Washington University School of Medicine, St. Louis, MO 63110
[4]Department of Medicine/Hematology and Oncology, University of Muenster, 48149 Muenster, Germany

Graft-versus-host disease (GVHD) causes significant morbidity and mortality in allogeneic hematopoietic stem cell transplantation (aHSCT), preventing its broader application to non–life-threatening diseases. We show that a single administration of a nondepleting monoclonal antibody specific for the coinhibitory immunoglobulin receptor, B and T lymphocyte associated (BTLA), permanently prevented GVHD when administered at the time of aHSCT. Once GVHD was established, anti-BTLA treatment was unable to reverse disease, suggesting that its mechanism occurs early after aHSCT. Anti-BTLA treatment prevented GVHD independently of its ligand, the costimulatory tumor necrosis factor receptor herpesvirus entry mediator (HVEM), and required BTLA expression by donor-derived T cells. Furthermore, anti-BTLA treatment led to the relative inhibition of CD4$^+$ forkhead box P3$^-$ (Foxp3$^-$) effector T cell (T eff cell) expansion compared with precommitted naturally occurring donor-derived CD4$^+$ Foxp3$^+$ regulatory T cell (T reg cell) and allowed for graft-versus-tumor (GVT) effects as well as robust responses to pathogens. These results suggest that BTLA agonism rebalances T cell expansion in lymphopenic hosts after aHSCT, thereby preventing GVHD without global immunosuppression. Thus, targeting BTLA with a monoclonal antibody at the initiation of aHSCT therapy might reduce limitations imposed by histocompatibility and allow broader application to treatment of non–life-threatening diseases.

CORRESPONDENCE
Kenneth M. Murphy:
kmurphy@wustl.edu

Abbreviations used: aHSCT, allogeneic hematopoietic stem cell transplantation; BLI, bioluminescence imaging; BMC, BM cell; BTLA, B and T lymphocyte associated; Foxp3, forkhead box P3; GVHD, graft-versus-host disease; GVT, graft versus tumor; HVEM, herpesvirus entry mediator; MCMV, murine CMV; TCD-BM, T cell–depleted BMC; T eff cell, CD4$^+$Foxp3$-$ effector T cell; T reg cell, CD4$^+$Foxp3$^+$ regulatory T cell.

Replacement of an abnormal lymphohematopoietic system by allogeneic hematopoietic stem cell transplantation (aHSCT) from a healthy donor is an effective treatment for many disorders of the hematopoietic system (Sykes and Nikolic, 2005; Copelan, 2006). Induction of a mixed hematopoietic donor-host chimerism can induce long-lasting tolerance to foreign tissues without the need for life-long immunosuppressive therapy (Kawai et al., 2008). aHSCT therapy has been improved by better donor identification (Petersdorf et al., 2004), more tolerable conditioning regimens (McSweeney et al., 2001), and enhanced supportive care. However, significant treatment-related morbidity and mortality from chemotherapy, radiotherapy, infections, and graft-versus-host disease (GVHD) remain significant clinical problems. Therefore, aHSCT is commonly indicated only for treatment of conditions where other treatment options are far inferior or lacking.

Costimulatory molecules of the CD28 and TNF families regulate GVHD, with inhibitory and activating receptors either decreasing or increasing its severity (Tamada et al., 2000; Blazar et al., 2003; Xu et al., 2007). B and T lymphocyte associated (BTLA) is an inhibitory immunoglobulin superfamily receptor, whose ligand is the TNF receptor herpesvirus entry mediator

J.C. Albring and M.M. Sandau contributed equally to this paper.

© 2010 Albring et al. This article is distributed under the terms of an Attribution–Noncommercial–Share Alike–No Mirror Sites license for the first six months after the publication date (see http://www.rupress.org/terms). After six months it is available under a Creative Commons License (Attribution–Noncommercial–Share Alike 3.0 Unported license, as described at http://creativecommons.org/licenses/by-nc-sa/3.0/).

The Rockefeller University Press $30.00
J. Exp. Med. Vol. 207 No. 12 2551-2559
www.jem.org/cgi/doi/10.1084/jem.20102017

Supplemental Material can be found at:
http://jem.rupress.org/content/suppl/2010/11/12/jem.20102017.DC1.html

The Journal of Experimental Medicine

Downloaded from jem.rupress.org on August 5, 2011

Published November 15, 2010

(HVEM) and which has only been examined in a nonirradiated model of chronic allostimulation without classical GVHD where donor cells lacking BTLA failed to persist (Hurchla et al., 2007). The role of BTLA in aHSCT using irradiated recipients, in which clinical symptoms and pathology similar to human GVHD develop, has not been examined.

RESULTS AND DISCUSSION

To determine the role of BTLA in the development of GVHD, we first examined WT and BTLA$^{-/-}$ donor mice (Watanabe et al., 2003) using a nonlethal parent-into-irradiated F1 model of aHSCT (Stelljes et al., 2008). In this model, GVHD results from partial MHC mismatch between H-2^{b} haplotype donor cells and lethally irradiated H-2$^{b/d}$ haplotype recipients. BM and splenocytes from WT or BTLA$^{-/-}$ mice on the C57BL/6 background were transferred into lethally irradiated CB6F1 recipients (Fig. 1 a). Transplantation of WT donor cells into CB6F1 recipients caused body weight loss of ~30% and clinical scores (Cooke et al., 1996) of ~3 that persisted for >40 d. BTLA$^{-/-}$ and WT donor cells caused similar GVHD, suggesting that BTLA does not normally regulate GVHD in this model. To test whether BTLA expressed by recipient mice might regulate GVHD in this model, we used BTLA$^{-/-}$ CB6F1 hosts as recipients of BTLA$^{-/-}$ BM and splenocytes (Fig. S1 a). BTLA$^{-/-}$ donor cells induced similar GVHD in BTLA$^{+/-}$ and BTLA$^{-/-}$ hosts, which is comparable to GVHD by WT donor cells (Fig. 1 a). Collectively, these data suggest that BTLA does not normally regulate GVHD.

Because BTLA generates inhibitory signals and functions in autoimmunity (Watanabe et al., 2003), malaria infection (Lepenies et al., 2007), and intestinal inflammation (Steinberg et al., 2008), we wondered whether harnessing the inhibitory effects of BTLA on the immune response by forced engagement would attenuate GVHD. To test this, we compared the effects of an agonistic nondepleting anti-BTLA monoclonal antibody (Hurchla et al., 2005; Lepenies et al., 2007), 6A6, administered at the time of aHSCT (Fig. 1 b) with an isotype control antibody, PIP, that recognizes bacterial GST (Gronowski et al., 1999). Mice treated with PIP showed similar progression of GVHD (Fig. 1, a and b), with clinical scores between 3 and 4 persisting for >140 d (Fig. S1 b). GVHD was associated with thickening of the lamina propria and muscularis, with severe inflammation and ulceration of

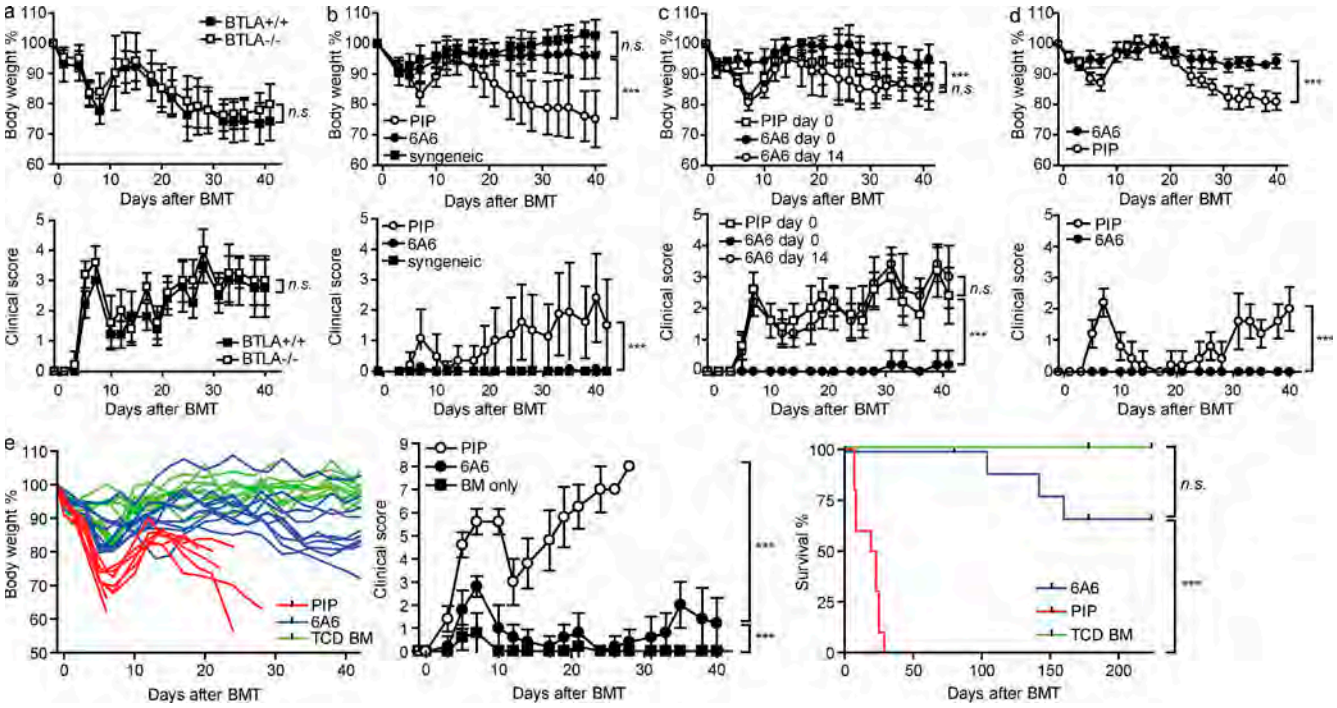

Figure 1. Anti-BTLA treatment permanently prevents GVHD. (a) Lethally irradiated CB6F1 mice received BMC and splenocytes from C57BL/6 WT (closed squares, $n = 5$) or BTLA$^{-/-}$ (open squares, $n = 5$) donors. (b) Lethally irradiated CB6F1 mice received BMC and splenocytes from syngeneic donors (closed squares, $n = 10$), C57BL/6 mice and antibodies PIP (open circles, $n = 15$), or 6A6 (closed circles, $n = 15$). Shown are cumulative data from three independent experiments. (c) Lethally irradiated CB6F1 mice received BMC and splenocytes from C57BL/6 mice plus control antibody PIP (open circles, $n = 5$) or 6A6 (closed circles, $n = 5$) on the day of BMT or 6A6 14 d after BMT (open squares, $n = 5$). (d) Lethally irradiated CB6F1 mice received BMC and splenocytes from C57BL/6 HVEM$^{-/-}$ mice and control antibody PIP (open circles, $n = 5$) or 6A6 (closed circles, $n = 5$). (e) Lethally irradiated BALB/c mice received TCD-BM alone (green lines and closed squares, $n = 10$) or in combination with splenocytes from C57BL/6 mice and control antibody PIP (red lines and open circles, $n = 10$) or 6A6 (blue lines and closed circles, $n = 10$) on the day of BMT. Shown are cumulative data from two independent experiments. Weight and clinical score data shown are mean ± SD. Data are representative of two independent experiments with five mice per group or cumulative data from independent experiments as indicated. P-values of >0.05 are considered not significant (n.s). ***, $P < 0.001$.

Downloaded from jem.rupress.org on August 5, 2011

Published November 15, 2010

the colon (Stelljes et al., 2008; Fig. S1 c, bottom). In contrast, a single treatment of 10 μg/g body weight of 6A6, given at the time of aHSCT, prevented GVHD completely, with weight loss and GVHD similar to the syngeneic control group (Fig. 1 b) for 140 d after aHSCT (Fig. S1 b). Furthermore, 6A6-treated mice had no histological evidence of GVHD in the colon (Fig. S1 c, top). Thus, a single administration of anti-BTLA antibody eliminates weight loss, histological changes, and clinical signs of GVHD.

We next asked if 6A6 acted by simply depleting donor cells that express BTLA. As a positive control, we included a depleting murine anti-BTLA antibody, 6F7 (Hurchla et al., 2005; Truong et al., 2009). CFSE-labeled donor cells were transferred into WT recipients that also received PIP, 6A6, or 6F7 antibody. 2 d after transfer, we found similar numbers of $CFSE^+$ cells in mice that received either PIP or 6A6 antibody (Fig. S1 d, left) and no significant differences between numbers of $CD19^+$, $CD4^+$, or $CD8^+$ lymphocytes (Fig. S1 d, right). Treatment with 6F7 caused a significant depletion of $CFSE^+$ lymphocytes, particularly from the $CD19^+$ cell population (Fig. S1 d). Furthermore, surface-bound 6A6 was detectable on live donor-derived cells in vivo up to 7 d after transfer (Fig. S1 e). In addition, 6A6 treatment was unable to prevent GVHD caused when $BTLA^{-/-}$ donors were used as a source of BM for aHSCT (Fig. S1 f). Thus, 6A6 does not deplete lymphocytes (Hurchla et al., 2007; Lepenies et al., 2007) but requires the expression of BTLA on donor cells to prevent GVHD.

Next, we asked if 6A6 could reverse established GVHD. We compared immediate with delayed administration of 6A6 (Fig. 1 c). Again, immediate 6A6 administration prevented GVHD. In contrast, there was no statistical difference in weight loss or clinical scores between mice that received 6A6 14 d after aHSCT and with mice that received PIP (Fig. 1 c).

6A6 binds to a region of BTLA that is involved in interactions with HVEM (Hurchla et al., 2005). Thus, 6A6 might prevent GVHD by preventing HVEM and BTLA interactions, thus blocking costimulatory signaling to donor cells (Xu et al., 2007). Although our data indicated that host BTLA is not involved (Fig. S1 a), we wished to test this possibility independently. Transfer of $HVEM^{-/-}$ donor cells caused induction of GVHD when administered with PIP (Fig. 1 d). The severity of GVHD caused by $HVEM^{-/-}$ donor cells was somewhat less than that caused by WT donor cells (Fig. 1 b), consistent with a study which found that HVEM and LIGHT are costimulatory in promoting GVHD (Xu et al., 2007). However, 6A6 also prevented GVHD caused by $HVEM^{-/-}$ donor cells (Fig. 1 d). These results indicate that 6A6 prevents GVHD in a manner that is independent of HVEM, suggesting it acts directly through BTLA.

Because the parent-into-irradiated F1 model of aHSCT does not result in lethal GVHD, we wished to test the potency of the anti-BTLA treatment in a model of complete MHC mismatch ($H\text{-}2^b$ into $H\text{-}2^d$) that results in lethal GVHD in untreated mice (Lu et al., 2001; Edinger et al., 2003b). Control mice developed severe GVHD with pronounced weight loss and clinical scores of >6 (Fig. 1 e, left and middle) and died within 30 d after aHSCT from severe GVHD (Fig. 1 e, right). Although mice that received the anti-BTLA treatment were not fully protected from GVHD, with clinical scores ranging from 1 to 3 (Fig. 1 e, middle) and slightly more weight loss than the control group that had received T cell–depleted BM cells (BMCs [TCD-BMs]) alone (Fig. 1 e, left), 70% of recipients treated with 6A6 survived for >200 d after aHSCT.

Although the precise molecular targets of BTLA signaling are still obscure (Gavrieli and Murphy, 2006; Wu et al., 2007), BTLA engagement by HVEM can inhibit T cell proliferation in vitro (Sedy et al., 2005) and promote tolerance induction in vivo (Liu et al., 2009). Therefore, we asked if anti-BTLA treatment alters donor T cell proliferation or IL-2 production in vivo. CFSE-labeled donor splenocytes were transferred into CB6F1 recipients that were treated with PIP, 6A6, or 6F7. Donor T cell proliferation was assessed after aHSCT and, by 3 d after aHSCT, reduced CFSE levels suggested that proliferation had occurred (Fig. 2 e). $CD4^+$ T cells had reduced proliferation after treatment with 6A6 and 6F7 antibodies 3 d after aHSCT (Fig. 2 e, middle), and the total accumulation of donor $CD4^+$ T cells was significantly reduced compared with control ($P < 0.0018$ and $P < 0.0083$; Fig. 2 b). In contrast, $CD8^+$ T cell proliferation and accumulation were not significantly affected by 6A6 treatment ($P < 0.8489$; Fig. 2, a and e, left). As 6F7 treatment leads to partial depletion of cells, we also assessed the level of annexin V binding, which is an indicator of early apoptosis. Mice treated with 6F7, but not PIP or 6A6, showed increased binding of annexin V on $CD4^+$ and $CD8^+$ T cells 7 d after aHSCT, which was not observed on day 3 (Fig. S1 g).

Although accumulation of $CD4^+$ T cells was lower in 6A6-treated than in PIP-treated mice, the production of IL-2 7 d after aHSCT was not statistically different (Fig. S2, a and b). A small but significant reduction in IFN-γ and IL-4, but not IL-17, production was observed in 6A6-treated mice compared with controls (Fig. S2, a and b). In summary, 6A6 administered at the time of aHSCT reduced the proliferation and accumulation of donor-derived $CD4^+Foxp3^-$ effector T cells (T eff cells) without inducing anergy, inhibiting IL-2 production or causing major alterations in cytokines.

These effects were suggestive of the actions of $CD4^+$ $Foxp3^+$ regulatory T cells (T reg cells) expressing the transcription factor forkhead box P3 (Foxp3; Hori et al., 2003). T reg cells have recently been reported to play a significant role in regulating GVHD (Taylor et al., 2002; Edinger et al., 2003b), and there are ongoing clinical trials aimed directly at the use of T reg cells as an intervention in human GVHD (NCI clinical trial NCT00725062).

To determine whether 6A6 treatment influences T reg cells, we measured the accumulation and proliferation of donor-derived T eff cells after aHSCT (Fig. 2, c and e, right). In PIP-treated recipients that developed GVHD, significantly fewer T reg cell were detected 7 d ($P < 0.0393$) after aHSCT when compared with recipients that received either anti-BTLA treatment 6A6 or 6F7 (Fig. 2 c). Therefore, anti-BTLA treatment inhibits the proliferation of T eff cells yet

Downloaded from jem.rupress.org on August 5, 2011

Published November 15, 2010

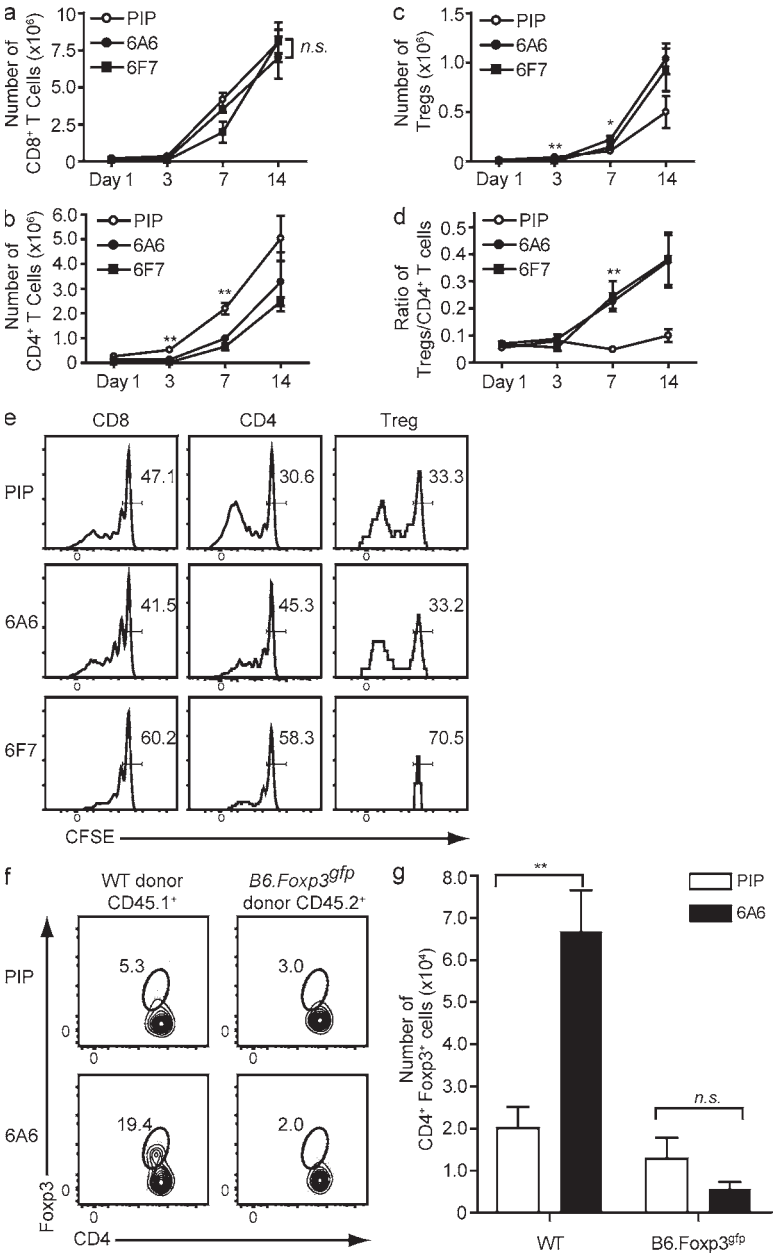

Figure 2. Anti-BTLA treatment allows for the expansion of preexisting donor-derived T reg cells by inhibiting T eff cell proliferation. (a–e) Lethally irradiated CB6F1 mice received a CFSE-labeled graft from B6.SJL donors and were treated with control antibody PIP (open circles), 6A6 (closed circles), or 6F7 (closed squares; $n = 3$ per group). The number of $CD8^+$ T cells (a), $CD4^+Foxp3^-$ (b), and $CD4^+$ $Foxp3^+$ (c) was calculated from absolute numbers of live splenocytes, and the percentage of the lymphocyte population was assayed by flow cytometry. (d) The ratio of total $CD4^+Foxp3^+/CD4^+Foxp3^-$ cells was calculated at the indicated time points by dividing the number of T reg cells in c by the number of T eff cells in b. (e) CFSE intensity of $CD8^+$, $CD4^+Foxp3^-$, and $CD4^+Foxp3^+$, 3 d after aHSCT with PIP, 6A6, or 6F7 treatment. (f and g) Lethally irradiated CB6F1 mice received aHSCT from B6.SJL mice along with purified $CD4^+$ Foxp3-negative T cells from *B6.Foxp3^{gfp}* mice with control antibody (PIP) or 6A6 ($n = 5$ per group). After 7 d, splenocytes were assayed by flow cytometry to determine the relative frequency of $CD4^+Foxp3^+$ cells among $CD4^+$ cells (f) or the absolute number of $CD4^+Foxp3^+$ T reg cells (g). Statistical comparisons in a–d are between the PIP- and 6A6-treated groups at the indicated time point, and the data are displayed as mean ± SEM. Shown are representative data from two independent experiments with three to five mice per group. P-values of >0.05 are considered not significant (n.s). *, $0.01 < P < 0.05$; **, $0.001 < P < 0.01$.

allows the accumulation of T reg cells, resulting in an increased T reg/T eff cell ratio ($P > 0.0028$; Fig. 2 d). This result is in agreement with the demonstration that T reg cells maintain low levels of BTLA after activation, in contrast to conventional T cells which up-regulate BTLA expression upon activation (Fig. S2 c; Hurchla et al., 2005). Thus, 6A6 treatment increases the numbers and the frequency of donor-derived T reg cells after aHSCT.

6A6 treatment could increase T reg cell frequency either by inducing Foxp3 expression in naive donor $CD4^+$ T cells (Chen et al., 2003) or by causing in vivo expansion of preexisting donor T reg cells relative to T eff cells. To distinguish these alternatives, we used *B6.Foxp3^{gfp}* reporter mice (Fontenot et al., 2005). We performed mixed aHSCT with WT and *Foxp3^{gfp}* mice as donors, using purified GFP-negative cells from *Foxp3^{gfp}* mice to remove preexisting T reg cells from the donor population. In this mixed aHSCT setting, 6A6 treatment similarly decreased the accumulation of T eff cells in both populations, but T reg cells expanded only from preexisting T reg cells (Fig. 2, f and g; and Fig. S2, e and f). Therefore, the donor T reg/T eff cell ratio increased only among the WT donor T cells and not in the *Foxp3^{gfp}* donor T cells, as assessed by intracellular staining for endogenous Foxp3 (Fig. 2 f and Fig. S2 g). In addition, donor-derived $CD4^+$ T cells, which were originally isolated from *B6.Foxp3^{gfp}* mice as negative for GFP expression, remained negative for Foxp3 as assessed by the Foxp3-GFP reporter (Fig. S2 e, right).

To further characterize the conditions necessary for the expansion of T reg cells, we evaluated what effects anti-BTLA treatment had on T reg cells in the steady state and whether the presence of alloantigen or HVEM on host tissue is required. When unmanipulated *B6.Foxp3^{gfp}* mice received 6A6, the frequency of T eff cells, T reg cells, or the resulting ratio did not change (Fig. S3, a–d). Similarly, although syngeneic aHSCT of CB6F1 resulted in a small decrease of T eff cells 7 d after transplant, no major accumulation of T reg cells and no increased T reg/T eff cell ratio was observed (Fig. S3, e–h). When $HVEM^{-/-}$ donors and MHC-mismatched $HVEM^{-/-}$ recipients were used, the ratio of T reg/T eff cells increased by inhibiting the accumulation of T eff cells

Downloaded from jem.rupress.org on August 5, 2011

Published November 15, 2010

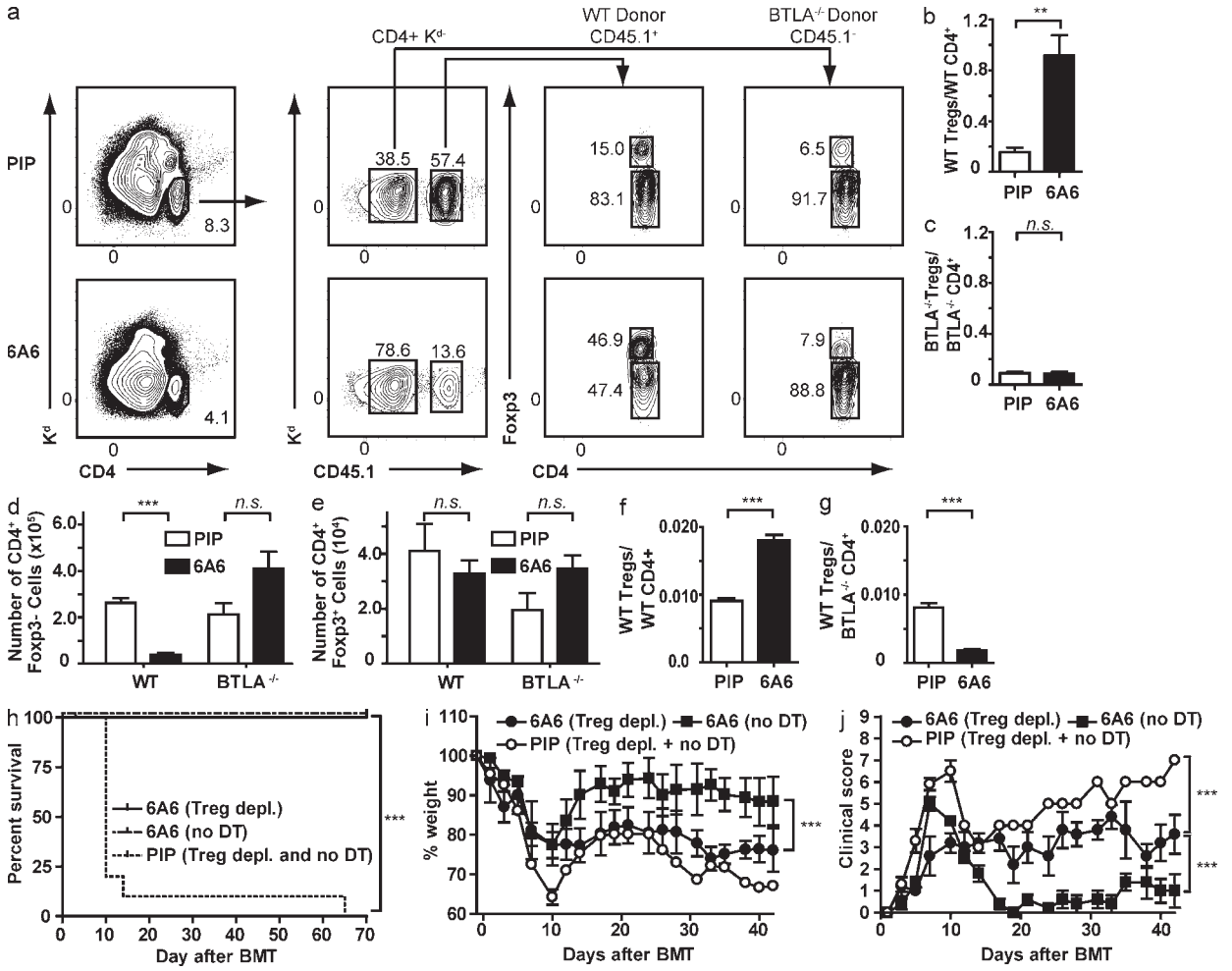

Figure 3. Direct engagement of BTLA on T eff cells leads to an increased frequency of CD4+Foxp3+ cells. Lethally irradiated CB6F1 mice received a 1:1 mixed aHSCT with WT-B6.SJL and B6 BTLA$^{-/-}$ donor cells (a–e) with either control antibody (PIP) or 6A6 (n = 5 per group). After 7 d, splenocytes were analyzed by flow cytometry. (a) Shown are FACS plots to identify donor cells as H-2K^{d-} and CD4+ (left). Intracellular Foxp3 was detected among CD4+ T cells (right) gated on WT-B6.SJL (CD4+CD45.1+ H-2K^{d-}) or B6 BTLA$^{+/+}$ (CD4+CD45.1− H-2K^{d-}) donor cell populations as indicated. Numbers represent the percentage of cells within the indicated gates. The ratios of the number of WT T reg/WT T eff cells (b) and KO T reg/ KO T eff cells (c) are shown, as well as the total number of T eff cells (d) and T reg cells (e) from the indicated donors after treatment with control antibody (PIP, open bars) or 6A6 (closed bars). (f and g) Lethally irradiated BALB/c mice received a 1:1 mixture of purified WT-B6.SJL and BTLA$^{-/-}$ CD4+ cells and T reg cells from *B6.Foxp3^{gfp}* mice, with either control antibody PIP or 6A6 (n = 3–4 per group). After 7 d, splenocytes were analyzed by flow cytometry to determine the ratio of WT T reg/WT T eff cells (f) or WT T reg/BTLA$^{-/-}$ T eff cells (g). Data are displayed as mean ± SEM. Shown are representative data from two independent experiments. (h–j) Recipient BALB/c mice received TCD-BM and splenocytes from T reg cell ablated or unmanipulated Foxp3^{DTR} mice and PIP or 6A6 as indicated. Survival curves (h), weight curves (i), and clinical scores (j) are shown for 6A6-treated mice that received a graft from either untreated (no DT) Foxp3^{DTR} donors (dashed line or filled squares; n = 5) or a graft from DT-treated (T reg depl.) Foxp3^{DTR} donors (solid line or filled circles; n = 5) and PIP-treated mice that received a graft from DT-treated or untreated (T reg depl. and no DT) Foxp3^{DTR} donors (dotted line or open circles; n = 10). Data are shown as mean ± SD from two independent experiments. P-values of >0.05 are considered not significant (n.s). **, 0.001 < P < 0.01; ***, P < 0.001.

(Fig. S3, i–l) as observed before (Fig. 2, d and g). Collectively, these results suggest that 6A6 has no effect in the steady state, does not involve HVEM, and requires allostimulation to increase the T reg/T eff cell ratio.

Because BTLA is expressed on both T eff and T reg cells, we tested whether the increased T reg/T eff cell ratio was the result of a decrease in T eff cell expansion, an increased proliferation of T reg cells, or both by performing a mixed aHSCT using congenically marked WT BTLA$^{+/+}$ and BTLA$^{-/-}$ donors. In this setting, the frequency of T reg cell within the CD4+BTLA$^{-/-}$ population did not change in the presence of 6A6 (7.9 ± 2 vs. 7.3 ± 2%; Fig. 3, a and c), whereas the T reg cell frequency within the CD4+ WT population increased more than threefold in the presence of 6A6 (48 ± 10 vs. 14.4 ± 5.5%; Fig. 3, a and b).

Importantly, 6A6 treatment decreased T eff cell numbers more than fivefold from $2.6 \times 10^5 \pm 4.6 \times 10^4$ cells in the control group to $3.9 \times 10^4 \pm 1.4 \times 10^4$ ($P < 0.0001$; Fig. 3 d), indicating that WT-BTLA$^{+/+}$ T eff cells are the main target of the anti-BTLA treatment. WT and BTLA$^{-/-}$ T reg cells

Downloaded from jem.rupress.org on August 5, 2011

Published November 15, 2010

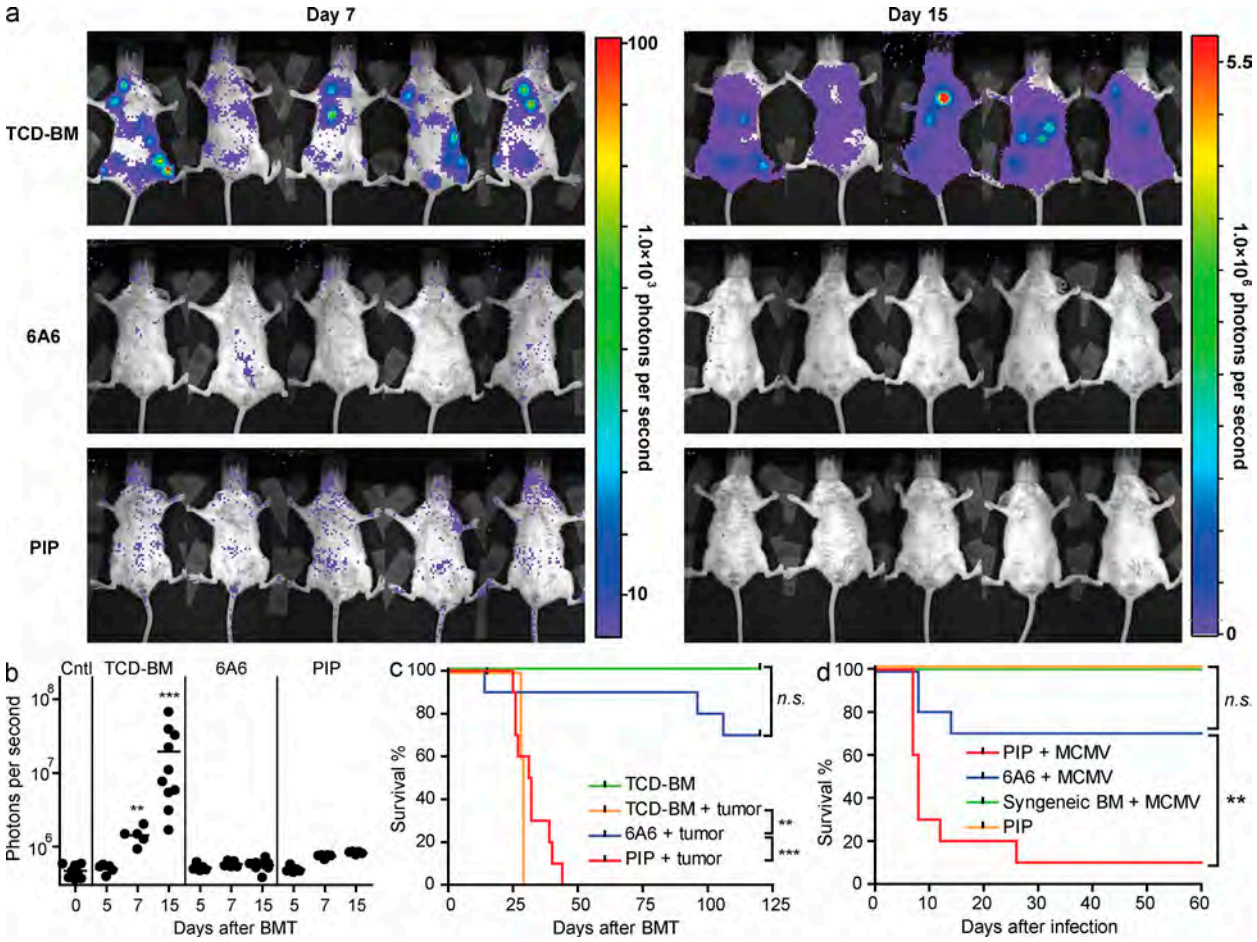

Figure 4. Anti-BTLA treatment does not lead to global immunosuppression. (a) Representative images of A20-Luc tumor cell localization 7 d (left) and 15 d (right) after aHSCT in lethally irradiated BALB/c mice that had received A20-Luc lymphoma cells with TCD-BM alone (n = 10) or together with splenocytes from C57BL/6 mice and control antibody PIP (n = 10) or 6A6 (n = 10). (b) Shown are units of photons per second for individual animals from panel a for days 5 (n = 5), 7 (n = 5), and 15 (n = 10) after aHSCT, as well as unmanipulated BALB/c mice (day 0, n = 12) for comparison. Asterisks indicate statistically significant differences between TCD-BM and 6A6 groups. Shown are cumulative data from two independent experiments, with each point representing the BLI signal from an individual mouse. Horizontal lines represent the mean BLI signal. Vertical lines serve to separate experimental groups. (c) Survival data of mice from a and from mice that received TCD-BM alone without tumor for comparison. Shown are cumulative data from two independent experiments. (d) CB6F1 BMC and splenocytes from syngeneic (green line; n = 10) or C57BL/6 donors and antibodies PIP (red line; n = 10) or 6A6 (blue line; n = 10) were infected with MCMV 4 wk after aHSCT and were monitored for survival. PIP-treated uninfected mice (orange line, n = 10) served as controls. Shown are cumulative data from two independent experiments. Data are shown as mean ± SD from two independent experiments. P-values of >0.05 are considered not significant (n.s). **, 0.001 < P < 0.01; ***, P < 0.001.

do not expand significantly in the presence of BTLA$^{-/-}$ T eff cells (Fig. 3 e), confirming our observation that T reg cells expand only when T eff cells express BTLA and are inhibited by 6A6. To exclude any indirect effects on host tissues, we cotransferred purified populations of WT T reg cells together with WT or BTLA$^{-/-}$ T eff cells into BALB/c recipients, which express an allele of BTLA not recognized by 6A6 (Fig. 3, f and g; and Fig. S4; Hurchla et al., 2005). The WT T reg/WT T eff cell ratio increased after 6A6 treatement (P < 0.0004; Fig. 3 f) as observed before (Fig. 2 g and Fig. 3 b). In contrast, when BTLA$^{-/-}$ T eff cells were present the WT T reg/BTLA$^{-/-}$ T eff cell ratio did not increase (Fig. 3 g), indicating that the expansion of T reg cells is caused by 6A6 reducing the expansion of T eff cells. In this setting, the WT T reg/BTLA$^{-/-}$ T eff cell ratio even decreased (Fig. 3 g and Fig. S4 i), suggesting that low expression levels of BTLA on T reg cells inhibits their expansion when proliferation of BTLA$^{-/-}$ T eff cells is not restricted.

To ask whether the inhibition of T eff cells had an effect on GVHD in the absence of T reg cells, we used C57BL/6 Foxp3^{DTR} mice as donors in the lethal model of GVHD. Pretreatment with diphtheria toxin reduced T reg cells by >95% in Foxp3^{DTR} donors. 90% of control animals died within 14 d of aHSCT, irrespective of whether or not the BM graft contained T reg cells (Fig. 3 h). All mice that were treated with the 6A6 antibody survived beyond day 70 (Fig. 3 h). Mice that received a graft with T reg cells and 6A6 eventually recovered to ∼90% of their starting weight (Fig. 3 i) and developed

Downloaded from jem.rupress.org on August 5, 2011

Published November 15, 2010

low-grade GVHD with scores ranging from 1 to 3, as seen before (Fig. 1 e). Mice that received a T reg cell–depleted graft and 6A6, however, recovered only 70–80% of their starting weight and had more severe GVHD scores ranging from 3 to 5 (Fig. 3 j). These data highlight that forced inhibition of T eff cells through BTLA (Fig. 3 d) is sufficient to prevent lethality. Nonetheless, the relative expansion of T reg cells (Fig. 3, b and f) bears biological significance, as they are required to protect the host from clinical GVHD (Fig. 3, i and j).

Because engagement of BTLA by 6A6 inhibited T eff cell proliferation, we wondered whether this treatment allowed for antigen-specific responses to tumors and pathogens. First, we examined whether graft-versus-tumor (GVT) activity was maintained after 6A6 treatment (Fig. 4, a–c). We used a model of minimal residual disease after aHSCT that utilizes bioluminescence imaging (BLI) of luciferase-expressing A20-Luc leukemia cells (H-2^d) in vivo (Edinger et al., 2003a). In this model, GVT activity requires cytolytic activity of T cells to control the tumor (Edinger et al., 2003b). Transplantation of A20-Luc leukemia cells with TCD-BM alone resulted in progressive tumor growth (Fig. 4, a and b). In mice that had received a T cell–containing graft with or without the 6A6 antibody, however, tumor was never detectable by BLI, suggesting that GVT effects were intact. Although all control mice died before day 45 of severe GVHD, 90% of 6A6-treated mice survived beyond day 90 (Fig. 4 c). To exclude any antibody-mediated antitumor effects, we confirmed that the 6A6 antibody does not bind to A20 cells, which was expected because of their BALB/c origin (Fig. S2 d). To document initial tumor engraftment, we quantified the total tumor number A20-GFP cells in the BM by flow cytometry 7 d after aHSCT (Fig. S3 m).

We next examined immune responses to murine CMV (MCMV; Nguyen et al., 2008) 4 wk after aHSCT. All animals that had undergone syngeneic aHSCT survived for >60 d after infection (Fig. 4 d). Of the mice in the allogeneic group that had received the PIP antibody, 70% died within 10 d of infection compared with 20% of the 6A6-treated mice. Thus, although 6A6 treatment prevents GVHD, it allows for resistance to MCMV, unlike PIP-treated control recipients.

To test the immune response against bacterial infection, animals were infected with the intracellular bacterium *Listeria monocytogenes*. 3 d after infection, animals that had received the PIP antibody had either higher ($P = 0.0005$ for liver and $P = 0.1816$ for spleen) or lower *L. monocytogenes* organ burdens ($P = 0.0227$ for liver and $P = 0.0059$ for spleen; Fig. S3, n–p), as has been described previously (Miura et al., 2000). In contrast, anti-BTLA–treated mice controlled infection similarly to both control groups, indicating an intact innate immune response (Fig. S3, n–p). These preliminary results suggest that 6A6-treated mice were similarly resistant to *L. monocytogenes* infection to unmanipulated mice.

In summary, this study demonstrates that the anti-BTLA antibody 6A6 administered at the time of aHSCT prevents GVHD without the need for additional immunosuppressive therapy. The mechanism of action is through direct engagement of BTLA on donor T cells, selectively inhibiting T eff cells and allowing the relative expansion of naturally occurring T reg cells. Once established, this new balance of T eff cells is sufficient to prevent GVHD permanently while allowing for intact responses to viral and bacterial pathogens, as well as GVT effects. Thus, BTLA may represent a novel therapeutic target in prevention of human GVHD. Increasing the safety of aHSCT could potentially allow its application more widely as a tolerogenic therapy in treatment of autoimmune disorders or solid organ transplantation, for which it is currently performed only experimentally (Sykes and Nikolic, 2005; Kawai et al., 2008).

MATERIALS AND METHODS

Mice and BM transplantation. B6.SJL-Ptprca Pep3b/BoyJ (B6.SJL), C57BL/6, and C57BL/6 × BALB/c F1 (CB6F1) mice were obtained from The Jackson Laboratory or bred in our facility. *BTLA*$^{-/-}$ (Watanabe et al., 2003), *Hvem*$^{-/-}$ (Wang et al., 2005), *Foxp3*^{gfp} (Fontenot et al., 2005), and *Foxp3*^{DTR} (Kim et al., 2007) mice were backcrossed to C57BL/6 for at least nine generations. HVEM$^{-/-}$ H2-K$^{b/d}$ or H2-K$^{d/d}$ were obtained by crossing HVEM$^{-/-}$ mice on a B6 (H2-K$^{b/b}$) background to BALB/c (H2-K$^{d/d}$) mice. The resulting HVEM$^{+/-}$ H2-K$^{d/b}$ F1 mice were intercrossed to obtain HVEM$^{-/-}$ H2-K$^{b/d}$ or H2-K$^{d/d}$ F2 recipients. Mice were 12–18 wk old and sex matched for all experiments. Mice were bred and maintained in our specific pathogen–free animal facility according to institutional guidelines with protocols approved by the Animal Studies Committee of Washington University.

Cell transplantation and assessment of GVHD. Mice received transplants according to a standard protocol as previously described (Stelljes et al., 2008). In brief, BMCs were harvested by flushing tibia and femurs of donor mice. For the nonlethal parent-into-F1 model of GVHD, CB6F1 (H-$2^{b/d}$) recipients were lethally irradiated with 9 Gy total body irradiation using a ^{137}Cs source at a dose rate of ∼70 cGy/min and reconstituted with 2×10^7 BMCs and 10^7 splenocytes from syngeneic (H-$2^{b/d}$) or parental C57BL/6 donors (H-2^b). For the lethal model of GVHD, BALB/c (H-2^d) recipients were lethally irradiated with 8 Gy total body irradiation using a ^{137}Cs source at a dose rate of ∼70 cGy/min and reconstituted with 2×10^7 TCD-BM alone or an additional 10^7 splenocytes from allogeneic C57BL/6 donors (H-2^b). To obtain TCD-BM, cells were depleted of CD4$^+$ and CD8$^+$ cells by magnetic depletion (Miltenyi Biotec) according to the manufacturer's recommendation. In experiments where a T reg cell–depleted graft from *Foxp3*^{DTR} donors was used, recipients received an intraperitoneal injection of 20 μg diphtheria toxin on the day of BMT. GVHD was monitored by calculating the loss in total body weight. Body weights were measured before transplantation and three times a week after transplantation. Clinical GVHD intensity was scored by assessing weight loss, posture, activity, fur texture, and skin integrity (Cooke et al., 1996). Histopathologic analyses of the bowel were performed on hematoxylin and eosin–stained tissue.

Administration of antibody. In some experiments, mice received at the time of aHSCT, unless otherwise noted, a single intraperitoneal injection of 10–20 μg/g body weight of anti-BTLA antibodies 6A6 and 6F7, whose properties we have previously published in detail (Hurchla et al., 2005). In brief, the IgG hamster monoclonal antibody 6A6 is specific for the C57BL/6 allele of BTLA and does not deplete BTLA-expressing cells in vivo (Hurchla et al., 2007; Lepenies et al., 2007). The IgG1κ mouse monoclonal anti-BTLA antibody 6F7 recognizes all known alleles of BTLA (Hurchla et al., 2005) and has been shown to deplete BTLA-expressing cells in vivo. The IgG1 hamster monoclonal anti-GST antibody PIP (Gronowski et al., 1999) was used as an isotype control.

Cell purification and depletion. To obtain purified populations of CD4$^+$ Foxp3^{gfp}-negative cells or CD4$^+$ Foxp3^{gfp}-positive cells in the indicated experiments, Foxp3^{gfp} splenocytes were stained with CD4$^+$ and the desired population was purified by cell sorting on the MoFlo cytometer (Dako).

Downloaded from jem.rupress.org on August 5, 2011

Published November 15, 2010

Purification of C57BL/6 $CD4^+$ and $BTLA^{-/-}$ $CD4^+$ cells was obtained from splenocytes that were depleted of $CD8^+$ and $B220^+$ cells by magnetic depletion (Miltenyi Biotech) according to the manufacturer's recommendation. *Foxp3*^{DTR} mice received intraperitoneal injections for 2 d of 20 µg diphtheria toxin per day before harvesting BM and splenocytes for aHSCT.

CFSE labeling and flow cytometry. Cells were labeled with CFSE (Sigma-Aldrich) by being incubated for 8 min at 25°C with 1 µM CFSE at a density of 40×10^6 cells per ml in PBS. Labeling was quenched by incubation of cells for 1 min with an equal volume of FCS and cells were washed twice with media containing 10% (vol/vol) FCS. 50×10^6 total cells per mouse were injected intravenously. Single cell suspensions from spleens were analyzed by flow cytometry using the following antibodies for detection: K^d-FITC (SF1-1.1), CD4-PECy7, APC, PerCPCy5.5, v450 (RM4-5) and PE (GK1.5), CD8-v450 (53–6.7), anti–Armenian and Syrian hamster IgG cocktail-PE, CD19-APC (1D3), and annexin V–PE (BD); and CD45.1-PECy7 and APC (A20), CD45.2-APC-eFluor780 (104), CD8-APC Alexa Fluor 750 (53–6.7), CD4-APC Alexa Fluor 750 (RM4-5), BTLA-bio (6F7), and SA-v450 (eBioscience). Intracellular Foxp3 was detected using the Mouse Regulatory T cell staining kit (eBioscience) with Foxp3-PE or APC (FJK-16s). For intracellular cytokine staining, splenocytes were first restimulated with PMA/ionomycin for 4 h and were stained with antibodies to surface markers, followed by fixation with 2% formaldehyde for 15 min at room temperature. Cells were then washed once in 0.05% saponin and stained with anti-cytokine antibodies (anti-IL-17 FITC, IL-2 PE, IFN-γ PE-Cy7, and IL-4 APC) in 0.5% saponin. All flow cytometry data were collected on a FACSCanto II (BD) and were analyzed with FlowJo software (Tree Star, Inc.).

Tumor model and assessment of GVT effects. As a tumor challenge, 2×10^4 A20-Luc or A20-GFP where administered intravenously together with the donor graft as indicated. Imaging was done as previously described (Rehemtulla et al., 2000; Edinger et al., 2003a). In brief, D-Luciferin (Biosynth AG) was reconstituted in 0.9% sodium chloride (Baxter) to a concentration of 15 mg/ml, filtered (0.2 µm), and frozen at −80°C until use. Mice were given intraperitoneal injections at a dose of 150 mg/kg and allowed to remain active in the cage for 5 min to allow circulation of luciferin. Using the Xenogen IVIS 200 system (Caliper Life Sciences) with attached anesthesia chamber, the animals were then anesthetized with 2% isoflurane for 5 min and subsequently transferred to the imaging chamber where they continued to receive a regulated flow of isoflurane through the manifold's nose cones. The Living Image software program (Caliper Life Sciences) was used to obtain and analyze data. For all experiments, a 60-s exposure time was used. To detect A20-GFP in the BM, single cell suspensions from both femurs were analyzed by flow cytometry using the antibody CD19-APC (1D3; BD). Cells that expressed high levels of CD19 and GFP were considered to be A20-GFP cells.

Cell lines. The BALB/c B cell lymphoma cell line A20 was obtained from the American Type Culture Collection. To generate luciferase-expressing A20 cells (A20-Luc), a 1995-bp HindIII–BamHI fragment from pGL4.23[luc2/minP] vector (Promega) containing a minimal promoter, a Luc2 coding sequence, and a SV40 late poly(A) signal was cloned into the HindIII and BamHI sites of the pcDNA3.1$^+$ mammalian expression vector (Invitrogen) to generate pcDNA3.1$^+$-Luc2. For stable transfections, 10×10^6 A20 cells/ml in complete IMDM supplemented with 10% fetal calf serum and with 30 µg/ml PvuI-linearized pcDNA3.1$^+$-Luc2 were electroporated at room temperature in 0.4-ml aliquots in 0.4-cm cuvettes in a Gene Pulser (Bio-Rad Laboratories) at 240 V and 960 mF. After electroporation, cells were cultured for 24 h in IMDM supplemented with 10% fetal calf serum and then selected in the presence of 800 µg/ml geneticin. To generate GFP-expressing A20 cells, a retroviral reporter vector (Ranganath et al., 1998) was used that contains the coding sequence of herpes simplex virus 1 thymidine kinase, followed by an internal ribosomal entry site and GFP (HSV1-TK-IRES-GFP-RV). The retroviral vector was packaged in Phoenix A cells. Before infection, the A20 cell line was stimulated with 5 µg/ml LPS (Sigma-Aldrich) for 24 h. For infection, cells were cultured in retroviral supernatant supplemented with 8 µg/ml polybrene (Sigma-Aldrich) and 5 µg/ml LPS and spun at 930 rcf for 1 h before being cultured at 37°C for 24 h. 72 h after infection, cells were sorted for high GFP expression on a FACSAria II (BD) and stable GFP expression of >95% was confirmed several times by flow cytometry at later time points.

Models of infectious disease. For MCMV infection, mice were infected with Smith strain MCMV 4 wk after aHSCT. Virus preparation and administration was performed as described previously (Krug et al., 2004). In brief, a salivary gland stock of MCMV was prepared from BALB/c mice, with a titer of 6.75×10^6 PFU/ml. Mice were infected intraperitoneally with a low dose of virus (10^4 PFU/mouse) and then monitored for survival. For *L. monocytogenes* infection, mice were infected intravenously with 2.5×10^4 *L. monocytogenes* (strain EGD; gift from E.R. Unanue, Washington University School of Medicine, St. Louis, MO) 3 mo after aHSCT. To determine organ *L. monocytogenes* burden at day 3 after infection, spleens and livers were homogenized in PBS plus 0.05% Triton X-100. Serial dilutions of homogenate were plated on brain heart infusion agar, and bacterial CFUs were assessed after overnight growth at 37°C. Small portions of spleen and liver were also fixed in 10% formalin and stained with hematoxylin and eosin.

Statistical analysis. A Student's unpaired two-tailed *t* test with a 95% confidence interval was used for statistical analyses of body weight data, clinical scores, and cell numbers. For analyses of survival data the log-rank test was used. A Mann-Whitney unpaired two-tailed Student's *t* test with a 95% confidence interval was used for statistical analyses of bioluminescence data in Fig. 4. Statistical analyses were done using Prism 4 (GraphPad Software, Inc.). FACS data are expressed as means ± SEM. All other data are presented as means ± SD. All experiments have been repeated at least once with three to five mice per group, unless stated otherwise.

Online supplemental material. Fig. S1 demonstrates that BTLA expression by recipient tissue does not promote GVHD and 6A6 antibody does not deplete lymphocytes. Fig. S2 shows that 6A6 treatment does not lead to donor T eff cell anergy and expands preexisting T reg cells. Fig. S3 shows that 6A6 inhibition of T eff cells and expansion of T reg cells requires allostimulation but not HVEM expression by donor or host. Fig. S4 shows that 6A6 alters the T reg cell/effector $CD4^+$ T cell ratio by directly inhibiting BTLA-expressing T cells. Online supplemental material is available at http://www.jem.org/cgi/content/full/jem.20102017/DC1.

The authors thank T.S. Stappenbeck for help with histology and T.R. Bradstreet for help with *L. monocytogenes* experiments.

K.M. Murphy is a Howard Hughes Medical Institute investigator. This work was supported in part by the National Institutes of Health (AI076427-02) and the Department of Defense (W81XWH-09-1-0185). J.C. Albring was supported by a German Research Foundation Grant (AL 1038/1-1). M.M. Sandau was supported by a Ruth L. Kirschstein National Reasearch Service Award (NIH # 5F32AI080062-02) and by the Irvington Institute Fellowship Program of the Cancer Research Institute. B.T. Edelson was supported by the Burroughs Wellcome Fund Career Award for Medical Scientists.

The authors have no conflicting financial interests.

Submitted: 24 September 2010
Accepted: 29 October 2010

REFERENCES

Blazar, B.R., B.M. Carreno, A. Panoskaltsis-Mortari, L. Carter, Y. Iwai, H. Yagita, H. Nishimura, and P.A. Taylor. 2003. Blockade of programmed death-1 engagement accelerates graft-versus-host disease lethality by an IFN-gamma-dependent mechanism. *J. Immunol.* 171:1272–1277.

Chen, W., W. Jin, N. Hardegen, K.J. Lei, L. Li, N. Marinos, G. McGrady, and S.M. Wahl. 2003. Conversion of peripheral $CD4^+CD25^-$ naive T cells to $CD4^+CD25^+$ regulatory T cells by TGF-β induction of transcription factor Foxp3. *J. Exp. Med.* 198:1875–1886. doi:10.1084/jem.20030152

Cooke, K.R., L. Kobzik, T.R. Martin, J. Brewer, J. Delmonte Jr., J.M. Crawford, and J.L.M. Ferrara. 1996. An experimental model of idiopathic pneumonia syndrome after bone marrow transplantation: I. The roles of minor H antigens and endotoxin. *Blood.* 88:3230–3239.

Downloaded from jem.rupress.org on August 5, 2011

Published November 15, 2010

Copelan, E.A. 2006. Hematopoietic stem-cell transplantation. *N. Engl. J. Med.* 354:1813–1826. doi:10.1056/NEJMra052638

Edinger, M., Y.A. Cao, M.R. Verneris, M.H. Bachmann, C.H. Contag, and R.S. Negrin. 2003a. Revealing lymphoma growth and the efficacy of immune cell therapies using in vivo bioluminescence imaging. *Blood.* 101:640–648. doi:10.1182/blood-2002-06-1751

Edinger, M., P. Hoffmann, J. Ermann, K. Drago, C.G. Fathman, S. Strober, and R.S. Negrin. 2003b. CD4+CD25+ regulatory T cells preserve graft-versus-tumor activity while inhibiting graft-versus-host disease after bone marrow transplantation. *Nat. Med.* 9:1144–1150. doi:10.1038/nm915

Fontenot, J.D., J.P. Rasmussen, L.M. Williams, J.L. Dooley, A.G. Farr, and A.Y. Rudensky. 2005. Regulatory T cell lineage specification by the forkhead transcription factor foxp3. *Immunity.* 22:329–341. doi:10.1016/j.immuni.2005.01.016

Gavrieli, M., and K.M. Murphy. 2006. Association of Grb-2 and PI3K p85 with phosphotyrosile peptides derived from BTLA. *Biochem. Biophys. Res. Commun.* 345:1440–1445. doi:10.1016/j.bbrc.2006.05.036

Gronowski, A.M., D.M. Hilbert, K.C.F. Sheehan, G. Garotta, and R.D. Schreiber. 1999. Baculovirus stimulates antiviral effects in mammalian cells. *J. Virol.* 73:9944–9951.

Hori, S., T. Nomura, and S. Sakaguchi. 2003. Control of regulatory T cell development by the transcription factor Foxp3. *Science.* 299:1057–1061. doi:10.1126/science.1079490

Hurchla, M.A., J.R. Sedy, M. Gavrieli, M. Gavrielli, C.G. Drake, T.L. Murphy, and K.M. Murphy. 2005. B and T lymphocyte attenuator exhibits structural and expression polymorphisms and is highly induced in anergic CD4+ T cells. *J. Immunol.* 174:3377–3385.

Hurchla, M.A., J.R. Sedy, and K.M. Murphy. 2007. Unexpected role of B and T lymphocyte attenuator in sustaining cell survival during chronic allostimulation. *J. Immunol.* 178:6073–6082.

Kawai, T., A.B. Cosimi, T.R. Spitzer, N. Tolkoff-Rubin, M. Suthanthiran, S.L. Saidman, J. Shaffer, F.I. Preffer, R.C. Ding, V. Sharma, et al. 2008. HLA-mismatched renal transplantation without maintenance immunosuppression. *N. Engl. J. Med.* 358:353–361. doi:10.1056/NEJMoa071074

Kim, J.M., J.P. Rasmussen, and A.Y. Rudensky. 2007. Regulatory T cells prevent catastrophic autoimmunity throughout the lifespan of mice. *Nat. Immunol.* 8:191–197. doi:10.1038/ni1428

Krug, A., A.R. French, W. Barchet, J.A.A. Fischer, A. Dzionek, J.T. Pingel, M.M. Orihuela, S. Akira, W.M. Yokoyama, and M. Colonna. 2004. TLR9-dependent recognition of MCMV by IPC and DC generates coordinated cytokine responses that activate antiviral NK cell function. *Immunity.* 21:107–119. doi:10.1016/j.immuni.2004.06.007

Lepenies, B., K. Pfeffer, M.A. Hurchla, T.L. Murphy, K.M. Murphy, J. Oetzel, B. Fleischer, and T. Jacobs. 2007. Ligation of B and T lymphocyte attenuator prevents the genesis of experimental cerebral malaria. *J. Immunol.* 179:4093–4100.

Liu, X.K., M. Alexiou, N. Martin-Orozco, Y. Chung, R.I. Nurieva, L. Ma, Q. Tian, G. Kollias, S. Lu, D. Graf, and C. Dong. 2009. Cutting edge: A critical role of B and T lymphocyte attenuator in peripheral T cell tolerance induction. *J. Immunol.* 182:4516–4520. doi:10.4049/jimmunol.0803161

Lu, Y., S. Sakamaki, H. Kuroda, T. Kusakabe, Y. Konuma, T. Akiyama, A. Fujimi, N. Takemoto, K. Nishiie, T. Matsunaga, et al. 2001. Prevention of lethal acute graft-versus-host disease in mice by oral administration of T helper 1 inhibitor, TAK-603. *Blood.* 97:1123–1130. doi:10.1182/blood.V97.4.1123

McSweeney, P.A., D. Niederwieser, J.A. Shizuru, B.M. Sandmaier, A.J. Molina, D.G. Maloney, T.R. Chauncey, T.A. Gooley, U. Hegenbart, R.A. Nash, et al. 2001. Hematopoietic cell transplantation in older patients with hematologic malignancies: replacing high-dose cytotoxic therapy with graft-versus-tumor effects. *Blood.* 97:3390–3400. doi:10.1182/blood.V97.11.3390

Miura, T., D. Mizuki, S. Sasaki, S. Hasegawa, H. Sashinami, and A. Nakane. 2000. Host resistance to *Listeria monocytogenes* infection is enhanced but resistance to *Staphylococcus aureus* infection is reduced in acute graft-versus-host disease in mice. *Infect. Immun.* 68:4340–4343. doi:10.1128/IAI.68.7.4340-4343.2000

Nguyen, V.H., S. Shashidhar, D.S. Chang, L. Ho, N. Kambham, M. Bachmann, J.M. Brown, and R.S. Negrin. 2008. The impact of regulatory T cells on T-cell immunity following hematopoietic cell transplantation. *Blood.* 111:945–953. doi:10.1182/blood-2007-07-103895

Petersdorf, E.W., C. Anasetti, P.J. Martin, T. Gooley, J. Radich, M. Malkki, A. Woolfrey, A. Smith, E. Mickelson, and J.A. Hansen. 2004. Limits of HLA mismatching in unrelated hematopoietic cell transplantation. *Blood.* 104:2976–2980. doi:10.1182/blood-2004-04-1674

Ranganath, S., W. Ouyang, D. Bhattarcharya, W.C. Sha, A. Grupe, G. Peltz, and K.M. Murphy. 1998. GATA-3-dependent enhancer activity in IL-4 gene regulation. *J. Immunol.* 161:3822–3826.

Rehemtulla, A., L.D. Stegman, S.J. Cardozo, S. Gupta, D.E. Hall, C.H. Contag, and B.D. Ross. 2000. Rapid and quantitative assessment of cancer treatment response using in vivo bioluminescence imaging. *Neoplasia.* 2:491–495. doi:10.1038/sj.neo.7900121

Sedy, J.R., M. Gavrieli, K.G. Potter, M.A. Hurchla, R.C. Lindsley, K. Hildner, S. Scheu, K. Pfeffer, C.F. Ware, T.L. Murphy, and K.M. Murphy. 2005. B and T lymphocyte attenuator regulates T cell activation through interaction with herpesvirus entry mediator. *Nat. Immunol.* 6:90–98. doi:10.1038/ni1144

Steinberg, M.W., O. Turovskaya, R.B. Shaikh, G. Kim, D.F. McCole, K. Pfeffer, K.M. Murphy, C.F. Ware, and M. Kronenberg. 2008. A crucial role for HVEM and BTLA in preventing intestinal inflammation. *J. Exp. Med.* 205:1463–1476. doi:10.1084/jem.20071160

Stelljes, M., S. Hermann, J. Albring, G. Köhler, M. Löffler, C. Franzius, C. Poremba, V. Schlösser, S. Volkmann, C. Opitz, et al. 2008. Clinical molecular imaging in intestinal graft-versus-host disease: mapping of disease activity, prediction, and monitoring of treatment efficiency by positron emission tomography. *Blood.* 111:2909–2918. doi:10.1182/blood-2007-10-119164

Sykes, M., and B. Nikolic. 2005. Treatment of severe autoimmune disease by stem-cell transplantation. *Nature.* 435:620–627. doi:10.1038/nature03728

Tamada, K., K. Shimozaki, A.I. Chapoval, G. Zhu, G. Sica, D. Flies, T. Boone, H. Hsu, Y.X. Fu, S. Nagata, et al. 2000. Modulation of T-cell-mediated immunity in tumor and graft-versus-host disease models through the LIGHT co-stimulatory pathway. *Nat. Med.* 6:283–289. doi:10.1038/73136

Taylor, P.A., C.J. Lees, and B.R. Blazar. 2002. The infusion of ex vivo activated and expanded CD4(+)CD25(+) immune regulatory cells inhibits graft-versus-host disease lethality. *Blood.* 99:3493–3499. doi:10.1182/blood.V99.10.3493

Truong, W., W.W. Hancock, J.C. Plester, S. Merani, D.C. Rayner, G. Thangavelu, K.M. Murphy, C.C. Anderson, and A.M. Shapiro. 2009. BTLA targeting modulates lymphocyte phenotype, function, and numbers and attenuates disease in nonobese diabetic mice. *J. Leukoc. Biol.* 86:41–51. doi:10.1189/jlb.1107753

Wang, Y., S.K. Subudhi, R.A. Anders, J. Lo, Y. Sun, S. Blink, Y. Wang, J. Wang, X. Liu, K. Mink, et al. 2005. The role of herpesvirus entry mediator as a negative regulator of T cell-mediated responses. *J. Clin. Invest.* 115:711–717.

Watanabe, N., M. Gavrieli, J.R. Sedy, J. Yang, F. Fallarino, S.K. Loftin, M.A. Hurchla, N. Zimmerman, J. Sim, X. Zang, et al. 2003. BTLA is a lymphocyte inhibitory receptor with similarities to CTLA-4 and PD-1. *Nat. Immunol.* 4:670–679. doi:10.1038/ni944

Wu, T.H., Y. Zhen, C. Zeng, H.F. Yi, and Y. Zhao. 2007. B and T lymphocyte attenuator interacts with CD3zeta and inhibits tyrosine phosphorylation of TCRzeta complex during T-cell activation. *Immunol. Cell Biol.* 85:590–595. doi:10.1038/sj.icb.7100087

Xu, Y., A.S. Flies, D.B. Flies, G. Zhu, S. Anand, S.J. Flies, H. Xu, R.A. Anders, W.W. Hancock, L. Chen, and K. Tamada. 2007. Selective targeting of the LIGHT-HVEM costimulatory system for the treatment of graft-versus-host disease. *Blood.* 109:4097–4104. doi:10.1182/blood-2006-09-047332

Downloaded from jem.rupress.org on August 5, 2011

Appendix #6: Defining the mechanisms of antigen presentation and specific dendritic cell subsets following DNA vaccination

CD8α$^+$ dendritic cells are required for CTL priming after DNA vaccination

Lijin Li[1], John Herndon[1], Peter S. Goedegebuure[1, 3], Timothy P. Fleming[1, 3], Kenneth M. Murphy[2], William E. Gillanders[1, 3]

[1] Department of Surgery, Washington University School of Medicine

[2] Department of Pathology and Immunology, Washington University School of Medicine

[3] The Alvin J. Siteman Cancer Center at Barnes-Jewish Hospital and Washington University School of Medicine

Key Words: DNA vaccine, dendritic cell, CD8 T cell

Correspondence should be addressed to:

William E. Gillanders, M.D.

Professor of Surgery

Washington University School of Medicine

660 South Euclid Avenue

Saint Louis, MO 63110

Tel: (314) 747-0072

Fax: (314) 454-5509

e-mail: gillandersw@wustl.edu

SUMMARY

DNA vaccines have tremendous potential for the treatment of human disease worldwide. However, the mechanism(s) of antigen presentation and specific dendritic cell subtypes involved following DNA vaccination remain to be defined. Some evidence suggests that DNA vaccines activate CTL by the direct transfection of dendritic cells (direct priming). In contrast, other evidence suggests that non-immune cells are transfected, and antigens are subsequently processed and presented by dendritic cells to activate CTL (cross-presentation). Importantly, only certain immune cells, such as certain $CD8\alpha^+$ and $CD103^+$ lineages of dendritic cells, are efficient in cross-presentation, and strategies to optimize DNA-based vaccines depend critically on the mechanism(s) of antigen presentation and specific dendritic cell subtypes involved. We recently generated *Batf3*$^{-/-}$ mice which lack development of the $CD8\alpha^+$ and $CD103^+$ lineages of dendritic cells, allowing us to test the role of these dendritic cell subtypes and cross-presentation in CTL priming following DNA vaccination. We find that CTL activation is selectively ablated in *Batf3*$^{-/-}$ mice following DNA vaccination. These data provide the strongest evidence to date that cross-presentation and $CD8\alpha^+$ dendritic cells are required for the generation of effective CTL immunity following DNA vaccination, with important implications for the rational development of DNA vaccines.

INTRODUCTION

The observation that direct administration of recombinant DNA can generate potent immune responses established the field of DNA vaccines in the early 1990s. Since that time, DNA vaccines have remained an area of intense research interest, and vaccines targeting infectious disease and cancer have progressed into clinical trials. Advantages of the DNA vaccine platform include the remarkable safety profile of DNA vaccines, the relative ease of manufacture relative to proteins and other biologics, and the ability to stimulate both humoral and cellular immunity [1]. Despite this intense interest in the DNA vaccine platform, the basic mechanism(s) of action by which DNA vaccines produce antigen-specific immunity remain to be defined. Specifically, it remains unclear how DNA vaccination leads to antigen presentation capable of eliciting CTL immunity, and what specific cell types are involved in this process.

DNA vaccines typically consist of bacterial plasmids encoding the antigen of interest under the transcriptional control of a strong viral promoter. DNA vaccines are injected into the muscle or skin, and delivery methods such as electroporation and gene gun have been used to enhance antigen expression. Although the encoded antigen is expressed primarily in myocytes or keratinocytes, bone marrow-derived APCs are required to present antigen to CTL following DNA vaccination [2-4]. Currently, experimental evidence supports two alternative pathways of antigen presentation to CTL following DNA vaccination. First, professional APC, such as migratory dendritic cells (DC) present in muscle or skin, might be directly transfected by plasmid DNA and present encoded antigens to CTL through endogenous processing pathways (direct priming). Alternatively, transfected myocytes or keratinocytes might produce the encoded

antigen, which would then be transferred to professional APC and presented to CTL through cross-presentation (cross-priming). Evidence to support both alternatives has been reported. In support of direct priming, migratory DC transfected with vaccine DNA can be detected in the draining lymph nodes [5], and migratory DC have been shown to induce cellular immunity [6]. Specific depletion of directly transfected migratory DC has been reported to ablate CTL responses measured *ex vivo* [7]. In contrast, Corr et al. used plasmids with tetracycline-responsive promoter elements and adoptive transfer to demonstrate the importance of cross-presentation [8], while Cho et al. came to similar conclusions using plasmids with tissue-specific promoters [9]. Defining the pathway(s) of antigen presentation following DNA vaccination will help facilitate the rational development of DNA vaccines.

Recently, lymph node-resident CD8α$^+$ DC have been implicated as a key DC subset involved in cross-presentation and CTL immunity following viral infection [10]. We recently identified *Batf3* as a key transcription factor controlling the development of CD8α$^+$ DC [11]. *Batf3*$^{-/-}$ mice have a selective loss of CD8α$^+$ and CD103$^+$ DC, without abnormalities in other hematopoietic cell types or architecture. DC from *Batf3*$^{-/-}$ mice are deficient in cross-presentation, and CTL responses to viral infection and syngeneic tumors are impaired in *Batf3*$^{-/-}$ mice. Thus, *Batf3*$^{-/-}$ mice represent a unique opportunity to study the relative role of cross-presentation and CD8α$^+$ DC following DNA vaccination.

RESULTS AND DISCUSSION

***Batf3*$^{-/-}$ mice represent an appropriate model for studying mechanisms of antigen presentation following DNA vaccination.** We used *Batf3*$^{-/-}$ mice to test for the requirement of CD8α^{+} DC in response to DNA vaccination *in vivo*. First, we analyzed the cell populations infiltrating the vaccine site 16 h after gene gun vaccination to confirm the relevance of this model. Histological examination demonstrates significant edema and leukocyte infiltration in both wildtype and *Batf3*$^{-/-}$ mice (Figure 1A). Further characterization of the vaccine site cellular infiltrate by flow cytometry (Figure 1B and C) reveals a significant increase in the number of CD11b^{+} Gr1^{+} neutrophils following DNA vaccination by gene gun. The number of CD11b^{+} Gr1^{-} monocytes also increases, while the number of CD11c^{+} DC remains unchanged, and the number of langerin^{+} DC decreases after gene gun vaccination. In all cases, there is no significant difference between wildtype and *Batf3*$^{-/-}$ mice, providing additional evidence that *Batf3*$^{-/-}$ mice represent an appropriate model for studying mechanisms of antigen presentation following DNA vaccination.

CTL activation is selectively ablated in *Batf3*$^{-/-}$ mice following DNA vaccination. To test for a requirement of CD8α^{+} DC in response to DNA vaccination, we vaccinated wildtype and *Batf3*$^{-/-}$ mice with an OVA DNA vaccine administered by either gene gun or *i.m.* injection plus electroporation. *Batf3*$^{-/-}$ mice failed to generate OVA-specific CTL responses, suggesting a defect in the CTL response to DNA vaccine independent of the route of administration (Figure 2A). We have previously demonstrated that DC from *Batf3*$^{-/-}$ mice are deficient in cross-presentation, and CTL responses to viral infection and syngeneic tumors are impaired in *Batf3*$^{-/-}$

mice [11]. To confirm that CTL responses are intact in *Batf3*$^{-/-}$ mice, and that the defect observed is a result of deficient cross-presentation, we vaccinated wildtype and *Batf3*$^{-/-}$ mice with the minimal OVA peptide epitope, SIINFEKL, which does not require cross-presentation to induce CD8$^+$ T cell responses. *Batf3*$^{-/-}$ mice were able to mount a robust CTL response to the SIINFEKL peptide vaccine, similar to their wildtype counterparts (Figure 2C). Similarly, antibody responses following DNA vaccination are not dependent on cross-presentation. Wildtype and *Batf3*$^{-/-}$ mice were vaccinated with an OVA plasmid or control vector by either gene gun or *i.m.* electroporation. Blood samples were collected at multiple times and the levels of serum OVA-specific antibody were measured by ELISA. There was no significant difference in total IgG, IgG_1 or IgG_{2a} antibody between wildtype and *Batf3*$^{-/-}$ mice (Figure 2D). Taken together, these results confirm the critical role of CD8α$^+$ DC in CTL immune responses, and provide the strongest evidence to date that cross-presentation is the predominant mechanism of antigen presentation following DNA vaccination.

Adoptive transfer of CD8α$^+$ DC partially rescues the CTL response to DNA vaccination in *Batf3*$^{-/-}$ mice. To confirm that selective ablation of the CTL response is related to the deficiency in CD8α$^+$ DC, rescue experiments were performed. CD8α$^+$ DC were isolated from wildtype mice spleens by FACS-sorting to a purity >90%, and adoptively transferred into *Batf3*$^{-/-}$mice 24 h prior to DNA vaccination (Figure 3A). The CTL response is significantly increased following adoptive transfer, confirming the central role of CD8α$^+$ DC following DNA vaccination (Figure 3B).

Previous studies implicating cross-presentation as a mechanism of antigen presentation following DNA vaccination relied on comparisons between ubiquitous and tissue-specific promoters [9, 12, 13]. Although evidence supports the tissue-specificity of the CD11c and K14 promoters [14], we have noticed that mRNA expression at the vaccine site is highly variable using these promoter constructs, and this introduces a potential confounder that limits mechanistic insights (data not shown). Several types of cells have been considered as APC in DNA vaccination. Langerhans cells form a dense network in the outermost layers of the skin [15], but the selective ablation of these cells did not prevent the induction of humoral or cell-mediated immune responses after DNA vaccination [16]. Likewise, B cells are unlikely to be the principal APC involved, since *ex vivo* responses generated using purified B cells as APC were significantly lower than responses using purified DC [12]. DCs have generally been implicated as APC in DNA vaccination. However, in mice in which class I MHC are expressed exclusively in DC (CD11c-MHCI), CTL responses to DNA vaccines were impaired but not ablated, suggesting the contribution of other APC in the response to DNA vaccination [13]. We do not specifically exclude the participation of other APC as accessory cells. However, it is also possible that the levels of class I MHC expression and subset distribution in CD11c-MHCI mice is lower than that required for effective cross-presentation or to support optimal CTL responses.

In mice, lymphoid tissue-resident $CD8\alpha^+$ DC have emerged as a key DC subset involved in cross-presentation, with the ability to present exogenous antigen onto major histocompatability type I molecules to elicit CTL responses [10, 11]. $CD8\alpha^+$ DC also express specific Toll-like receptor and C-type lectin pattern recognition receptors, and can efficiently phagocytose dying cells [17]. A DC subset with similar phenotype and function has recently been identified in

humans [18-21]. The studies presented here confirm the importance of CD8α$^+$ DC in the CTL response to DNA vaccination, providing strong evidence for the importance of cross-presentation. These studies have important implications for ongoing efforts to optimize the efficacy of the DNA vaccine platform. Previous efforts have focused on delivery of antigen to DEC-205$^+$ DC [22]. Our studies suggest that targeting CD8α$^+$ DC may be more productive. Alternatively, strategies aimed at enhancing cross-presentation are likely to be effective.

MATERIALS AND METHODS

Animals. Generation of *Batf3*$^{-/-}$ mice on the 129SvEv background was described previously [11]. All mice were bred and maintained in specific pathogen-free animal facilities according to institutional guidelines. Protocols were approved by the Animal Studies Committee at Washington University School of Medicine.

Antibodies and flow cytometry. Fluorochrome-labeled monoclonal antibodies were purchased from BD, eBioscience, BioLegend, Miltenyi Biotec, and Dendritics. Antibody staining was generally performed in the presence of Fc block (BD). All flow cytometry data were collected on FACSCalibur instruments (BD) and analyzed using the FlowJo software (TreeStar).

DNA and peptide immunization. Full-length OVA cDNA was cloned into the pcDNA3.1(+) vector (Invitrogen) using standard techniques and was confirmed by DNA sequencing. DNA was administered by gene gun (intradermal) or by electroporation (*i.m.*) at 3-day intervals for a total of three doses. Primary immune responses were examined five days after the final vaccination. For gene gun immunization, 4 μg of DNA was delivered to non-overlapping depilated abdominal skin. The discharge helium pressure of the Helios gene gun (Bio-Rad) was set to 400 p.s.i.. For electroporation, DNA was delivered using the TriGrid Delivery System (Ichor Medical Systems). 10 μg of DNA (20 μL) was injected (*i.m.*) followed by the application of a pre-programmed electric current. For peptide vaccination, 40 μg of SIINFEKL peptide (AnaSpec) was mixed with the adjuvant TiterMax Gold (Sigma-Aldrich) and injected (*s.c.*) at the dorsal tail base.

ELISPOT and intracellular cytokine staining. IFN-γ ELISPOT assay was performed with reagents purchased from Mabtech unless otherwise noted. Briefly, 96-well PVDF filtration plates (Millipore) were coated overnight with 15 µg/mL of capture antibody. Erythrocyte-free single spleen cell suspensions were added in triplicate and incubated for 20 hr with or without the presence of 1 µM SIINFEKL peptide (AnaSpec). After extensive washes, 1 µg/mL of biotinylated detection antibody was added. Streptavidin-ALP and BCIP/NBT (Moss Substrates) were subsequently used for color development. Plates were scanned and analyzed on an ImmunoSpot reader (C.T.L.). For intracellular IFN-γ staining, splenocytes were cultured *ex vivo* in the presence of GolgiPlug (BD) and 1 µM SIINFEKL. Cells were harvested 24 h later and stained for CD8 followed by intracellular IFN-γ staining.

Anti-OVA ELISA. 96-well microtiter plates (Corning) were coated with 150 µg/mL OVA (Sigma-Aldrich) and blocked. 100 µL of immune sera (diluted 1:200) was added and incubated for 2 h. The plates were washed and HRP-conjugated goat anti-mouse IgG, IgG_1 or IgG_{2a} (Southern Biotech, diluted 1:5000) were added and incubated for 1.5 h. The amount of bound OVA-specific Ab was determined by measuring the absorbance at 450 nm with a microplate reader (Bio-Rad Model 550) after colorimetric development using TMB substrate solution (Moss Substrates).

Dendritic cell sorting and adoptive transfer. Spleens were minced, and digested with 1 mg/mL collagenase D and 0.002% DNase I (both from Roche) for 45 minutes at 37ºC. Single cell

suspensions were subjected to further DC enrichment using the I-Mag DC enrichment kit (BD) following the manufacturer's instructions. The purity of the enriched $CD11c^+$ DC preparations was >75%. $CD11c^+CD8\alpha^+$ DC were sorted on a MoFlo instrument (Beckman Coulter) and adoptively transferred into *Batf3*$^{-/-}$ mice.

Histology of the vaccine sites. 16 hours after gene gun bombardment, skin tissues from the vaccine sites were excised and fixed in 10% buffered formalin. Five-micron cross sections of the paraffin-embedded tissues were stained with hematoxylin and eosin. Skin from naïve mice were harvest and processed to serve as control (0 h). To determine the nature of the cellular infiltrates, skin tissues were digested in 5 mg/mL dispase (StemCell Technology) followed by 1 mg/mL collagenase D (Roche). Cells were harvested using cell scrapers and passed through 100-µm strainers prior to staining and analysis for the cell surface CD11b, CD11c, Gr-1 and intracellular Langerin (CD207) antigens by flow cytometry.

Data analysis. Data were analyzed using Prism 5 (GraphPad Software). An unpaired, two-tailed Student's *t*-test was used to compare differences between groups, with $P \leq 0.05$ considered significant. Figures were exported and prepared using Adobe Illustrator CS3 (Adobe Systems).

ACKNOWLEDGEMENTS

We thank Ted Hansen for helpful discussions.

This work was supported in part by the Department of Defense Breast Cancer Research Program Grant W81XWH-06-1-0677 and by a Postdoctoral Fellowship Award to Lijin Li.

CONFLICT OF INTEREST

There are no financial or commercial conflicts of interest.

REFERENCES

1 **Kutzler, M. A. and Weiner, D. B.,** DNA vaccines: ready for prime time? *Nat Rev Genet* 2008. **9**: 776-788.

2 **Corr, M., Lee, D. J., Carson, D. A. and Tighe, H.,** Gene vaccination with naked plasmid DNA: mechanism of CTL priming. *J Exp Med* 1996. **184**: 1555-1560.

3 **Doe, B., Selby, M., Barnett, S., Baenziger, J. and Walker, C. M.,** Induction of cytotoxic T lymphocytes by intramuscular immunization with plasmid DNA is facilitated by bone marrow-derived cells. *Proc Natl Acad Sci U S A* 1996. **93**: 8578-8583.

4 **Iwasaki, A., Torres, C. A., Ohashi, P. S., Robinson, H. L. and Barber, B. H.,** The dominant role of bone marrow-derived cells in CTL induction following plasmid DNA immunization at different sites. *J Immunol* 1997. **159**: 11-14.

5 **Condon, C., Watkins, S. C., Celluzzi, C. M., Thompson, K. and Falo, L. D., Jr.,** DNA-based immunization by in vivo transfection of dendritic cells. *Nat Med* 1996. **2**: 1122-1128.

6 **Klinman, D. M., Sechler, J. M., Conover, J., Gu, M. and Rosenberg, A. S.,** Contribution of cells at the site of DNA vaccination to the generation of antigen-specific immunity and memory. *J Immunol* 1998. **160**: 2388-2392.

7 **Porgador, A., Irvine, K. R., Iwasaki, A., Barber, B. H., Restifo, N. P. and Germain, R. N.,** Predominant role for directly transfected dendritic cells in antigen presentation to CD8+ T cells after gene gun immunization. *J Exp Med* 1998. **188**: 1075-1082.

8 **Corr, M., von Damm, A., Lee, D. J. and Tighe, H.,** In vivo priming by DNA injection occurs predominantly by antigen transfer. *J Immunol* 1999. **163**: 4721-4727.

9 **Cho, J. H., Youn, J. W. and Sung, Y. C.,** Cross-priming as a predominant mechanism for inducing CD8(+) T cell responses in gene gun DNA immunization. *J Immunol* 2001. **167**: 5549-5557.

10 **Shortman, K. and Heath, W. R.,** The CD8+ dendritic cell subset. *Immunol Rev* 2010. **234**: 18-31.

11 **Hildner, K., Edelson, B. T., Purtha, W. E., Diamond, M., Matsushita, H., Kohyama, M., Calderon, B., Schraml, B. U., Unanue, E. R., Diamond, M. S., Schreiber, R. D., Murphy, T. L. and Murphy, K. M.,** Batf3 deficiency reveals a critical role for CD8alpha+ dendritic cells in cytotoxic T cell immunity. *Science* 2008. **322**: 1097-1100.

12 **Hon, H., Oran, A., Brocker, T. and Jacob, J.,** B lymphocytes participate in cross-presentation of antigen following gene gun vaccination. *J Immunol* 2005. **174**: 5233-5242.

13 **Lauterbach, H., Gruber, A., Ried, C., Cheminay, C. and Brocker, T.,** Insufficient APC capacities of dendritic cells in gene gun-mediated DNA vaccination. *J Immunol* 2006. **176**: 4600-4607.

14 **Lin, M. T., Wang, F., Uitto, J. and Yoon, K.,** Differential expression of tissue-specific promoters by gene gun. *Br J Dermatol* 2001. **144**: 34-39.

15 **Romani, N., Holzmann, S., Tripp, C. H., Koch, F. and Stoitzner, P.,** Langerhans cells - dendritic cells of the epidermis. *Apmis* 2003. **111**: 725-740.

16 **Stoecklinger, A., Grieshuber, I., Scheiblhofer, S., Weiss, R., Ritter, U., Kissenpfennig, A., Malissen, B., Romani, N., Koch, F., Ferreira, F., Thalhamer, J. and Hammerl, P.,** Epidermal langerhans cells are dispensable for humoral and cell-mediated immunity elicited by gene gun immunization. *J Immunol* 2007. **179**: 886-893.

17 **Sancho, D., Joffre, O. P., Keller, A. M., Rogers, N. C., Martinez, D., Hernanz-Falcon, P., Rosewell, I. and Reis e Sousa, C.,** Identification of a dendritic cell receptor that couples sensing of necrosis to immunity. *Nature* 2009. **458**: 899-903.

18 **Bachem, A., Guttler, S., Hartung, E., Ebstein, F., Schaefer, M., Tannert, A., Salama, A., Movassaghi, K., Opitz, C., Mages, H. W., Henn, V., Kloetzel, P. M., Gurka, S. and**

Kroczek, R. A., Superior antigen cross-presentation and XCR1 expression define human CD11c+CD141+ cells as homologues of mouse CD8+ dendritic cells. *J Exp Med* 2010. **207**: 1273-1281.

19 **Crozat, K., Guiton, R., Contreras, V., Feuillet, V., Dutertre, C. A., Ventre, E., Vu Manh, T. P., Baranek, T., Storset, A. K., Marvel, J., Boudinot, P., Hosmalin, A., Schwartz-Cornil, I. and Dalod, M.,** The XC chemokine receptor 1 is a conserved selective marker of mammalian cells homologous to mouse CD8alpha+ dendritic cells. *J Exp Med* 2010. **207**: 1283-1292.

20 **Jongbloed, S. L., Kassianos, A. J., McDonald, K. J., Clark, G. J., Ju, X., Angel, C. E., Chen, C. J., Dunbar, P. R., Wadley, R. B., Jeet, V., Vulink, A. J., Hart, D. N. and Radford, K. J.,** Human CD141+ (BDCA-3)+ dendritic cells (DCs) represent a unique myeloid DC subset that cross-presents necrotic cell antigens. *J Exp Med* 2010. **207**: 1247-1260.

21 **Poulin, L. F., Salio, M., Griessinger, E., Anjos-Afonso, F., Craciun, L., Chen, J. L., Keller, A. M., Joffre, O., Zelenay, S., Nye, E., Le Moine, A., Faure, F., Donckier, V., Sancho, D., Cerundolo, V., Bonnet, D. and Reis e Sousa, C.,** Characterization of human DNGR-1+ BDCA3+ leukocytes as putative equivalents of mouse CD8alpha+ dendritic cells. *J Exp Med* 2010. **207**: 1261-1271.

22 **Bonifaz, L. C., Bonnyay, D. P., Charalambous, A., Darguste, D. I., Fujii, S., Soares, H., Brimnes, M. K., Moltedo, B., Moran, T. M. and Steinman, R. M.,** In vivo targeting of antigens to maturing dendritic cells via the DEC-205 receptor improves T cell vaccination. *J Exp Med* 2004. **199**: 815-824.

FIGURE LEGENDS

Figure 1. *Batf3*$^{-/-}$ mice generate a normal inflammatory infiltrate at the vaccine site following DNA vaccination. (A) Light microscopy of hematoxylin and eosin stained sections of skin tissues before (0 h) and 16 h after gene gun bombardment. Specimens from 2-4 animals from each group were examined and representative images are shown. Scale bar = 100 μm. (B) Flow cytometry evaluation of the inflammatory infiltrate at the DNA vaccine site. Cells harvested from the skin tissue of the vaccine sites were analyzed by flow cytometry and representative contour plots are shown. Numbers represent the frequencies of the gated populations. (C) Quantification of selected leukocyte subsets infiltrating the vaccine site. Frequencies of each subset among the indicated gate are shown. Insert: total number of CD11c^{+} langerin^{+} cells per 3 cm^{2} of skin. * $P < 0.01$.

Figure 2. CTL activation is selectively ablated in *Batf3*$^{-/-}$ mice following DNA vaccination. WT and *Batf3*$^{-/-}$ mice (n = 5 in each group) were immunized with OVA plasmid DNA by gene gun. Five days after the final vaccination, CTL responses were measured by IFN-γ ELISPOT (A) and intracellular cytokine staining (B). . The results are representative of at least two independent experiments. (C) WT and *Batf3*$^{-/-}$ mice were vaccinated by *s.c.* injection of SIINFEKL peptide (40 μg) prepared in the adjuvant TiterMax Gold. Control vaccines consisted of adjuvant mixed only with PBS. Seven days later, spleen cells were harvested and the number of IFN-γ-producing cells was measured in an ELISPOT assay. There is no significant difference in SFCs between WT and *Batf3*$^{-/-}$ mice. (D) WT and *Batf3*$^{-/-}$ mice were vaccinated with OVA DNA or empty vector at days 1 and 28. DNA was administered via gene gun (upper row) or *i.m.* electroporation

(lower row). Sera were collected prior to and after vaccination at multiple time points. Serum levels of OVA-specific antibody were measured by ELISA. Total IgG, IgG_1 and IgG_{2a} were equivalent between WT and *Batf3*$^{-/-}$ mice. *$P < 0.01$; ns: not significant.

Figure 3. Adoptive transfer of CD8α$^+$ DC partially rescues the CTL response to DNA vaccination in *Batf3*$^{-/-}$ mice. (A) CD8α$^+$ DC were isolated from *Batf3*$^{+/+}$ spleens by FACS-sorting to a purity >90%. 1.2×10^5 cells were adoptively transferred into *Batf3*$^{-/-}$ mice (n = 4) 24 h before DNA vaccination. (B) The CTL response was measured by IFN-γ ELISPOT, indicating a significant increase in the CD8$^+$ T cell response (*$P < 0.01$).

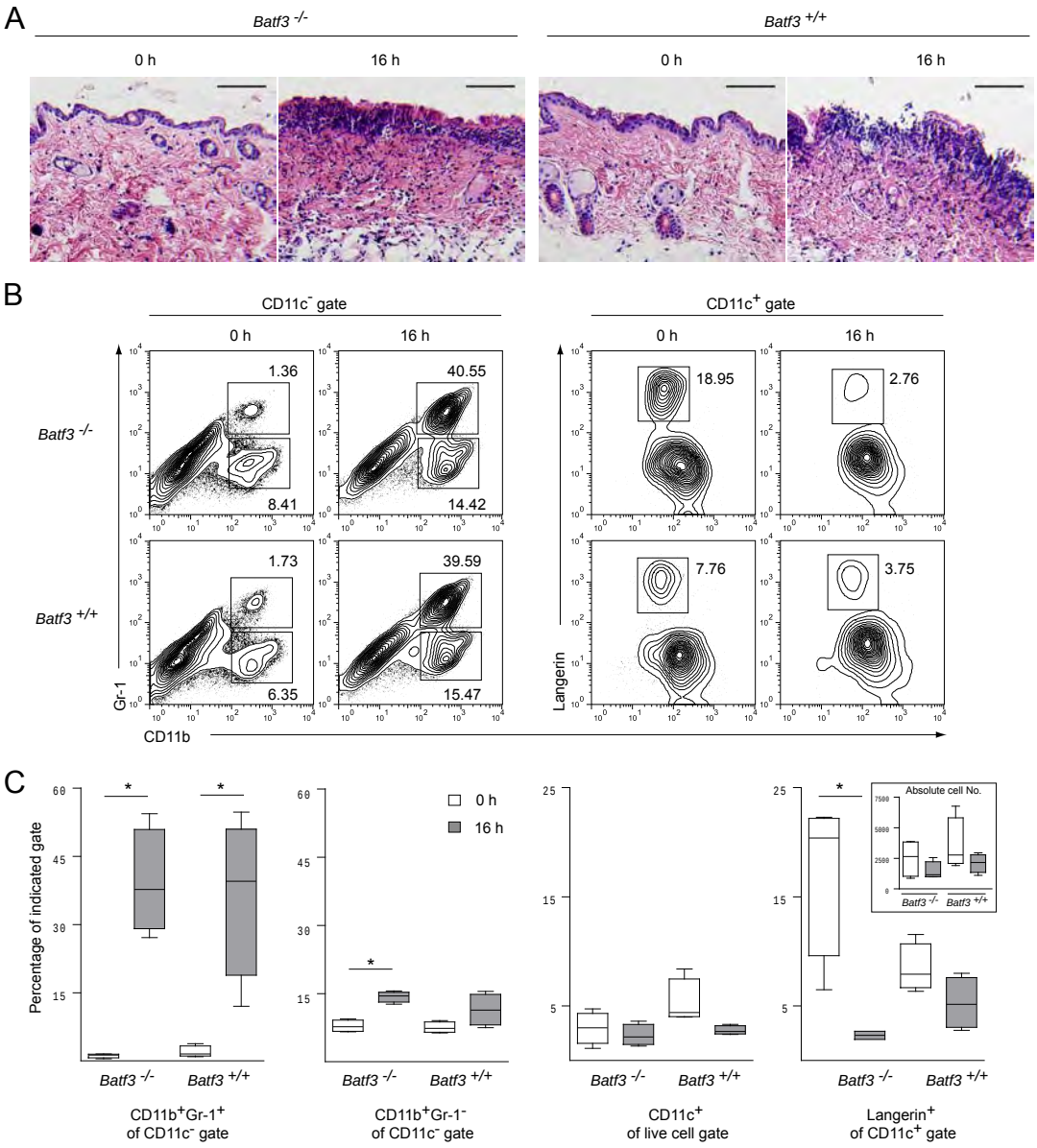
A
Batf3 -/-
Batf3 +/+
0 h
16 h
B
CD11c- gate
CD11c+ gate
Batf3 -/-
Batf3 +/+
1.36
40.55
8.41
14.42
1.73
39.59
6.35
15.47
18.95
2.76
7.76
3.75
Gr-1
CD11b
Langerin
C
Percentage of indicated gate
0 h
16 h
Absolute cell No.
CD11b+Gr-1+ of CD11c- gate
CD11b+Gr-1- of CD11c- gate
CD11c+ of live cell gate
Langerin+ of CD11c+ gate

Figure 1

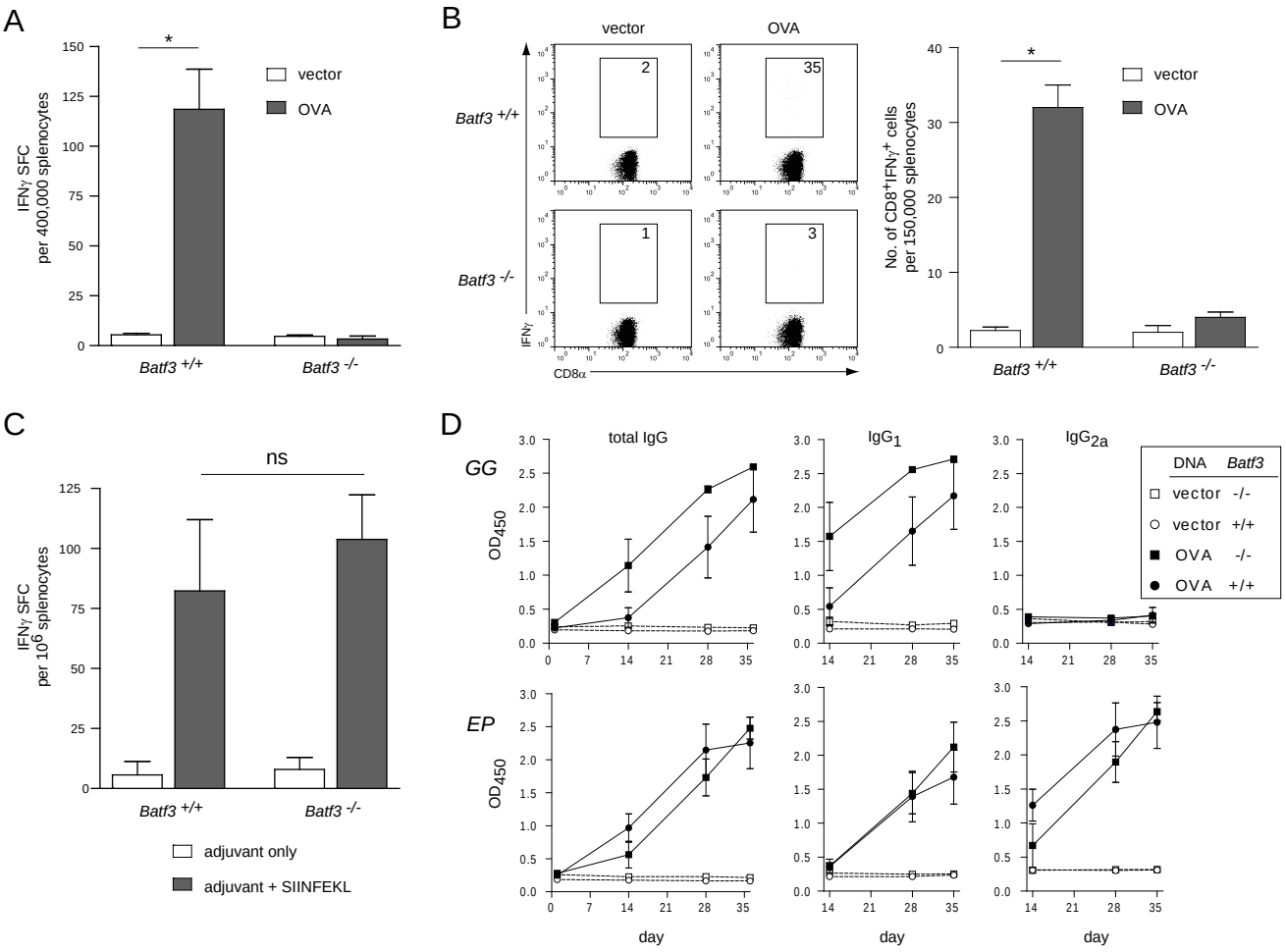
A
B
C
D
vector
OVA
Batf3 +/+
Batf3 -/-
IFNγ SFC per 400,000 splenocytes
No. of CD8+IFNγ+ cells per 150,000 splenocytes
IFNγ
CD8α
ns
IFNγ SFC per 10^6 splenocytes
adjuvant only
adjuvant + SIINFEKL
total IgG
IgG1
IgG2a
GG
EP
OD450
day
DNA Batf3
vector -/-
vector +/+
OVA -/-
OVA +/+

Figure 2

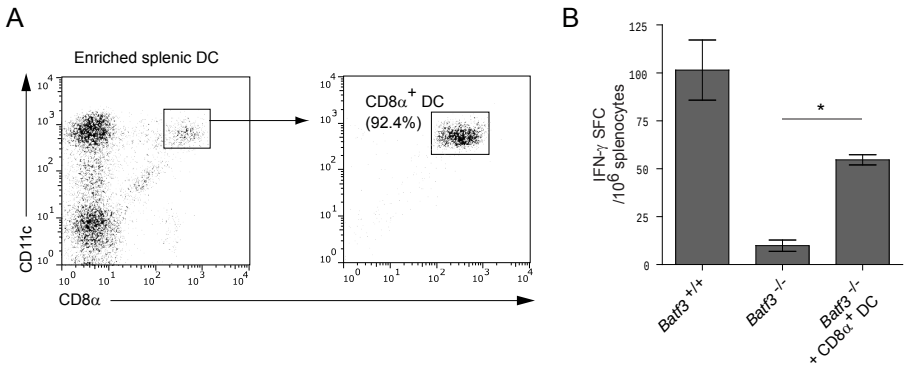
A
Enriched splenic DC
CD11c
CD8α
CD8α+ DC
(92.4%)
B
IFN-γ SFC
/10^6 splenocytes
125
100
75
50
25
0
*
Batf3 +/+
Batf3 -/-
Batf3 -/-
+ CD8α+ DC

Figure 3